

2014-144 _____ BWR Vessel & Internals Project (BWRVIP)

October 15, 2014

Document Control Desk
U. S. Nuclear Regulatory Commission
11555 Rockville Pike
Rockville, MD 20852

Attention: Joseph Holonich

Subject: Project No. 704 – BWRVIP-281NP: BWR Vessel and Internals Project,
Testing and Evaluation of the Perry 177° Capsule

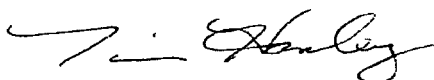
Enclosed are five (5) paper copies of the report “BWRVIP-281NP: BWR Vessel and Internals Project, Testing and Evaluation of the Perry 177° Capsule,” EPRI Technical Report 3002003141, October 2014. This report is being transmitted to the NRC for information only.

This report describes testing and evaluation of the Perry 177° capsule. These results will be used to monitor embrittlement as part of the BWRVIP ISP.

Please note that the enclosed report is non-proprietary and is available to the public by request to EPRI.

If you have any questions on this subject please call Ron DiSabatino (Exelon Corp., BWRVIP Assessment Focus Group Chairman) at 717-456-3685.

Sincerely,



Andrew McGehee, EPRI, BWRVIP Program Manager
Tim Hanley, Exelon Corporation, BWRVIP Chairman

c: S. Rosenberg, NRC-NRR
M. Kirk, NRC-RES
G. Stevens, NRC-RES
D. Odell, Exelon Corp.
R. Carter, EPRI
A. McGehee, EPRI
C. Wirtz, EPRI

Together . . . Shaping the Future of Electricity

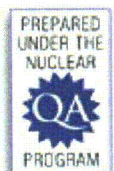
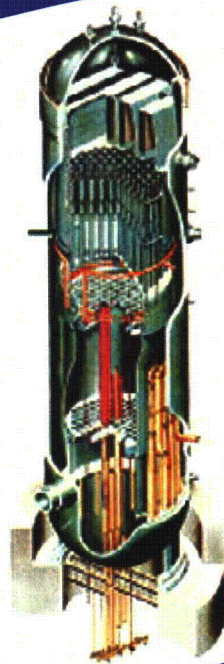
PALO ALTO OFFICE
3420 Hillview Avenue, Palo Alto, CA 94304-1395 USA • 650.855.2000 • Customer Service 800.313.3774 • www.epri.com

Extra copies were sent to the PM

*GOOD
NRR*

BWVRVIP-281NP: BWR Vessel and Internals Project

Testing and Evaluation of the Perry 177° Capsule



BWRVIP-281NP: BWR Vessel and Internals Project

*Testing and Evaluation of the Perry 177°
Capsule*

All or a portion of the requirements of the EPRI Nuclear
Quality Assurance Program apply to this product.



EPRI Project Manager
R. Carter

EPRI | ELECTRIC POWER
RESEARCH INSTITUTE

3420 Hillview Avenue
Palo Alto, CA 94304-1338
USA

PO Box 10412
Palo Alto, CA 94303-0813
USA

800.313.3774
650.855.2121

askpri@epri.com

www.epri.com

3002003141

Final Report, October 2014

DISCLAIMER OF WARRANTIES AND LIMITATION OF LIABILITIES

THIS DOCUMENT WAS PREPARED BY THE ORGANIZATION(S) NAMED BELOW AS AN ACCOUNT OF WORK SPONSORED OR COSPONSORED BY THE ELECTRIC POWER RESEARCH INSTITUTE, INC. (EPRI). NEITHER EPRI, ANY MEMBER OF EPRI, ANY COSPONSOR, THE ORGANIZATION(S) BELOW, NOR ANY PERSON ACTING ON BEHALF OF ANY OF THEM:

(A) MAKES ANY WARRANTY OR REPRESENTATION WHATSOEVER, EXPRESS OR IMPLIED, (I) WITH RESPECT TO THE USE OF ANY INFORMATION, APPARATUS, METHOD, PROCESS, OR SIMILAR ITEM DISCLOSED IN THIS DOCUMENT, INCLUDING MERCHANTABILITY AND FITNESS FOR A PARTICULAR PURPOSE, OR (II) THAT SUCH USE DOES NOT INFRINGE ON OR INTERFERE WITH PRIVATELY OWNED RIGHTS, INCLUDING ANY PARTY'S INTELLECTUAL PROPERTY, OR (III) THAT THIS DOCUMENT IS SUITABLE TO ANY PARTICULAR USER'S CIRCUMSTANCE; OR

(B) ASSUMES RESPONSIBILITY FOR ANY DAMAGES OR OTHER LIABILITY WHATSOEVER (INCLUDING ANY CONSEQUENTIAL DAMAGES, EVEN IF EPRI OR ANY EPRI REPRESENTATIVE HAS BEEN ADVISED OF THE POSSIBILITY OF SUCH DAMAGES) RESULTING FROM YOUR SELECTION OR USE OF THIS DOCUMENT OR ANY INFORMATION, APPARATUS, METHOD, PROCESS, OR SIMILAR ITEM DISCLOSED IN THIS DOCUMENT.

REFERENCE HEREIN TO ANY SPECIFIC COMMERCIAL PRODUCT, PROCESS, OR SERVICE BY ITS TRADE NAME, TRADEMARK, MANUFACTURER, OR OTHERWISE, DOES NOT NECESSARILY CONSTITUTE OR IMPLY ITS ENDORSEMENT, RECOMMENDATION, OR FAVORING BY EPRI.

THE FOLLOWING ORGANIZATIONS PREPARED THIS REPORT:

Electric Power Research Institute (EPRI)

MP Machinery & Testing LLC

TransWare Enterprises Inc.

THE TECHNICAL CONTENTS OF THIS PRODUCT WERE PREPARED IN ACCORDANCE WITH THE EPRI QUALITY PROGRAM MANUAL THAT FULFILLS THE REQUIREMENTS OF 10 CFR 50 APPENDIX B. THIS PRODUCT IS SUBJECT TO THE REQUIREMENTS OF 10 CFR PART 21. CERTIFICATION OF CONFORMANCE CAN BE OBTAINED FROM EPRI.

NOTE

For further information about EPRI, call the EPRI Customer Assistance Center at 800.313.3774 or e-mail askepri@epri.com.

Electric Power Research Institute, EPRI, and TOGETHER...SHAPING THE FUTURE OF ELECTRICITY are registered service marks of the Electric Power Research Institute, Inc.

Copyright © 2014 Electric Power Research Institute, Inc. All rights reserved.

Acknowledgments

The following organizations prepared this report:

Electric Power Research Institute (EPRI)
3420 Hillview Ave.
Palo Alto, CA 94304

Principal Investigators
N. Palm
T. Hardin

MP Machinery & Testing LLC
2161 Sandy Drive
State College, PA 16803

Principal Investigator
M.P. Manahan, Sr.

TransWare Enterprises Inc.
1565 Mediterranean Drive
Sycamore, IL 60178

Principal Investigator
E. Jones

This report describes research sponsored by EPRI and its BWRVIP participating members.

This publication is a corporate document that should be cited in the literature in the following manner:

BWRVIP-28 INP: BWR Vessel and Internals Project, Testing and Evaluation of the Perry 177° Capsule. EPRI, Palo Alto, CA: 2014. 3002003141.

Product Description

In the late 1990s, a Boiling Water Reactor Vessel and Internals Project (BWRVIP) Integrated Surveillance Program (ISP) was developed to improve the surveillance of the U.S. BWR fleet. This report describes testing and evaluation of the Perry Nuclear Power Plant (PNPP) 177° capsule. These results will be used to monitor embrittlement as part of the BWRVIP ISP.

Background

The BWRVIP ISP represents a major enhancement to the process of monitoring embrittlement for the U.S. fleet of BWRs. The ISP optimizes surveillance capsule tests while at the same time maximizing the quantity and quality of data, thus resulting in a more cost-effective program. The BWRVIP ISP provides more representative data that can be used to assess embrittlement in reactor pressure vessel beltline materials and improve trend curves in the BWR range of irradiation conditions.

Challenges and Objectives

Neutron irradiation exposure reduces the toughness of reactor vessel steel plates, welds, and forgings. The objectives of this project were twofold:

- To document the results of neutron dosimetry and Charpy V-notch ductility tests for the surveillance materials (plate heat C2557-1 and weld heat 5P6214B) in the Perry 177° capsule
- To compare the results with the embrittlement trend prediction of the U.S. Nuclear Regulatory Commission (U.S. NRC) Regulatory Guide 1.99, Rev. 2

Approach

The Perry 177° capsule had been irradiated in the reactor since plant startup. The surveillance capsule contained flux wires for neutron flux monitoring, Charpy V-notch impact test specimens, and tensile specimens. The project team removed the capsule from the reactor in 2013 and transported it to facilities for testing and evaluation. The team used dosimetry to gather information about the neutron fluence accrual of specimens from the capsule. They then performed a neutron transport calculation in accordance with Regulatory Guide 1.190 and compared it to the results from the dosimetry. Testing of

Charpy V-notch specimens was performed according to the American Society for Testing and Materials (ASTM) standards.

Results and Findings

The report includes capsule neutron exposure and Charpy V-notch test results for Perry surveillance plate heat C2557-1 and surveillance weld heat 5P6214B. The project compared irradiated Charpy data to unirradiated data in order to determine the shifts in Charpy index temperatures for the surveillance plate and weld materials due to irradiation. For the surveillance plate, the measured shift is less than the predicted shift + margin using Regulatory Guide 1.99, Revision 2. For the surveillance weld, the measured shift is greater than the predicted shift + margin using Regulatory Guide 1.99, Revision 2. Researchers also measured flux wires, determined fluence for the 177° capsule, and calculated a revised fluence for the previously tested 3° capsule.

Applications, Value, and Use

Results of this work will be used in the BWRVIP ISP that integrates individual BWR surveillance programs into a single program. The ISP provides data of high quality to monitor BWR vessel embrittlement. The ISP results in significant cost savings to the BWR fleet and provides more accurate monitoring of embrittlement in BWR vessels.

Keywords

BWR
Charpy testing
Mechanical properties
Radiation embrittlement
Reactor pressure vessel integrity
Reactor vessel surveillance program

Table of Contents

Section 1: Introduction	1-1
1.1 Implementation Requirements	1-2
Section 2: Materials and Test Specimen Description.....	2-1
2.1 Dosimeters	2-1
2.2 Test Materials	2-1
2.2.1 Capsule Loading Inventory.....	2-1
2.2.2 Material Description.....	2-4
2.2.3 Chemical Composition	2-5
2.2.4 CVN Baseline Properties	2-5
2.2.5 Tanh Curve Fits of CVN Test Data for Plate Heat C2557-1	2-10
2.2.6 Tanh Curve Fits of CVN Test Data for Weld Heat 5P6214B.....	2-12
2.3 Capsule Opening	2-14
Section 3: Neutron Fluence Calculation	3-1
3.1 Description of the Reactor System	3-2
3.1.1 Reactor System Mechanical Design.....	3-2
3.1.2 Reactor System Material Compositions.....	3-4
3.1.3 Reactor Operating Data Inputs	3-5
3.2 Calculation Methodology.....	3-9
3.2.1 Description of the RAMA Fluence Methodology.....	3-9
3.2.2 RAMA Geometry Model for the Perry Reactor	3-10
3.2.3 RAMA Calculation Parameters	3-18
3.2.4 RAMA Neutron Source Calculation.....	3-19
3.2.5 RAMA Fission Spectra	3-19
3.3 Surveillance Capsule Activation and Fluence Results	3-19
3.3.1 Comparison of Predicted Activation to Plant- specific Measurements	3-20
3.3.2 Capsule Peak Fluence Calculations and Lead Factor Determinations.....	3-22

3.4 Capsule Fluence Uncertainty Analysis.....	3-23
3.4.1 Comparison Uncertainty	3-24
3.4.2 Analytic Uncertainty	3-24
3.4.3 Combined Uncertainty.....	3-25
Section 4: Charpy Test Data.....	4-1
4.1 Charpy Test Procedure.....	4-1
4.2 Charpy Test Data for 177° Capsule	4-3
Section 5: Charpy Test Results	5-1
5.1 Analysis of Impact Test Results	5-1
5.2 Irradiated Versus Unirradiated CVN Properties.....	5-1
Section 6: References	6-1
Appendix A: Dosimeter Analysis	A-1
A.1 Dosimeter Material Description.....	A-1
A.2 Dosimeter Cleaning and Mass Measurement	A-1
A.3 Radiometric Analysis.....	A-2

List of Figures

Figure 2-1 Drawing Showing the Charpy Test Specimen Geometry and ASTM E23 Permissible Variations	2-2
Figure 2-2 Photograph of the 177° Perry Capsule (top) and a Magnified View of the External Identification Markings (bottom)	2-3
Figure 2-3 Photograph of the Inside of the 177 Degree Perry Capsule Showing the Dosimetry Location During the Irradiation	2-4
Figure 2-4 Charpy Energy Data for Plate Heat C2557-1 (TL) Unirradiated.....	2-10
Figure 2-5 Charpy Energy Data for Weld Heat 5P6214B Unirradiated.....	2-12
Figure 3-1 Planar View of Perry at the Core Mid-plane Elevation	3-3
Figure 3-2 Planar View of the Perry RAMA Quadrant Model at the Core Mid-plane Elevation.....	3-11
Figure 3-3 Axial View of the Perry RAMA Model.....	3-12
Figure 4-1 Illustration of Digital Optical Comparator Measurement of Shear Fracture Area	4-2
Figure 5-1 Irradiated Plate Heat C2557-1 Charpy Energy Plot (Perry 177° Capsule).....	5-2
Figure 5-2 Irradiated Weld Heat 5P6214B Charpy Energy Plot (Perry 177° Capsule).....	5-4
Figure 5-3 Irradiated Plate C2557-1 Lateral Expansion Plot (Perry 177° Capsule).....	5-6
Figure 5-4 Irradiated Weld Heat 5P6214B Lateral Expansion Plot (Perry 177° Capsule)	5-8

Figure A-1 Perry 177° Capsule Cu Dosimeter Wire Cu-1:
Prior to Cleaning (left); and After Cleaning/Coiling
(right) A-3

Figure A-2 Perry 177° Capsule Cu Dosimeter Wire Cu-2:
Prior to Cleaning (left); and After Cleaning/Coiling
(right) A-3

Figure A-3 Perry 177° Capsule Fe Dosimeter Wire Fe-1:
Prior to Cleaning (left); and After Cleaning/Coiling
(right) A-4

Figure A-4 Perry 177° Capsule Fe Dosimeter Wire Fe-2:
Prior to Cleaning (left); and After Cleaning/Coiling
(right) A-4

List of Tables

Table 2-1 Perry 177° Surveillance Capsule Specimen Inventory	2-2
Table 2-2 Best Estimate Chemistry of Available Data Sets for Plate Heat C2557-1	2-5
Table 2-3 Best Estimate Chemistry of Available Data Sets for Weld Heat 5P6214B.....	2-5
Table 2-4 Unirradiated Transverse Charpy V-Notch Impact Test Results for Surveillance Base Metal (Heat C2557-1) Specimens from the Perry Surveillance Program	2-6
Table 2-5 Unirradiated Longitudinal Charpy V-Notch Impact Test Results for Surveillance Base Metal (Heat C2557-1) Specimens from the Perry Surveillance Program.....	2-7
Table 2-6 Unirradiated Charpy V-Notch Impact Test Results for Surveillance Weld Metal (Heat 5P6214B, Lot 0331, Linde 124 Flux, Single Wire) Specimens from the Perry Surveillance Program.....	2-7
Table 2-7 Unirradiated Charpy V-Notch Impact Test Results for Surveillance Weld Metal (Heat 5P6214B, Lot 0331, Linde 124 Flux) Specimens from the Supplemental Surveillance Program (SSP).....	2-8
Table 2-8 Baseline CVN Properties.....	2-9
Table 3-1 Summary of Material Compositions by Region for Perry.....	3-5
Table 3-2 Summary of Perry Core Loading Inventory	3-7
Table 3-3 State-point Data for Each Cycle of Perry	3-8
Table 3-4 Comparison of Specific Activities for Perry Cycle 1 3° Flux Wire Holder Wires (C/M)	3-20
Table 3-5 Comparison of Specific Activities for Perry Cycle 5 3° Surveillance Capsule Flux Wires (C/M).....	3-21

Table 3-6 Comparison of Specific Activities for Perry Cycle 14 177° Surveillance Capsule Flux Wires (C/M).....	3-22
Table 3-7 Comparison of Activities for Perry Flux Wires.....	3-22
Table 3-8 Calculated Capsule Fast Neutron Fluence and Lead Factors for Perry.....	3-23
Table 3-9 Perry Capsule Uncertainty for Energy >1.0 MeV	3-25
Table 4-1 Irradiated Charpy V-Notch Impact Test Results for Surveillance Base Metal Specimens (Heat C2557-1) from the Perry 177° Surveillance Capsule.....	4-4
Table 4-2 Irradiated Charpy V-Notch Impact Test Results for Surveillance Weld Metal Specimens (Heat 5P6214B) from the Perry 177° Surveillance Capsule.....	4-5
Table 4-3 Irradiated Charpy V-Notch Impact Test Results for Surveillance HAZ Metal Specimens from the Perry 177° Surveillance Capsule	4-5
Table 5-1 Effect of Irradiation (E>1.0 MeV) on the Notch Toughness Properties	5-10
Table 5-2 Comparison of Actual Versus Predicted Embrittlement.....	5-11
Table 5-3 Percent Decrease In Upper Shelf Energy	5-11
Table A-1 Perry 177° Capsule Charpy Packet Dosimeter Wire Masses	A-4
Table A-2 Gamma Ray Spectrometer System (GRSS) Specifications	A-5
Table A-3 Counting Schedule for Perry 177° Capsule Dosimeter Materials.....	A-5
Table A-4 Neutron-Induced Reactions of Interest.....	A-5
Table A-5 Results of Perry 177° Capsule Radiometric Analysis.....	A-6

Section 1: Introduction

Test coupons of reactor vessel ferritic beltline materials are irradiated in reactor surveillance capsules to facilitate evaluation of vessel fracture toughness in vessel integrity evaluations. The key values that characterize fracture toughness are the reference temperature of nil-ductility transition (RT_{NDT}) and the upper shelf energy (USE). These are defined in 10CFR50 Appendix G [1] and in Appendix G of the ASME Boiler and Pressure Vessel Code, Section XI [2]. Appendix H of 10CFR50 [1] and ASTM E185-82 [3] establish the methods to be used for testing of surveillance capsule materials.

In the late 1990s the BWR Vessel and Internals Project (BWRVIP) initiated the BWRVIP Integrated Surveillance Program (ISP) [4], and the BWRVIP assumed responsibility for testing and evaluation of ISP capsules. The surveillance plate and weld from Perry Nuclear Power Plant (hereinafter, Perry) were designated as "ISP representative surveillance materials" to be tested by the ISP according to an approved capsule withdrawal and test schedule.

This report addresses the withdrawal and test of the Perry 177° surveillance capsule. The capsule contained flux wires for neutron flux monitoring, Charpy V-notch impact test specimens, and tensile specimens. The capsule was irradiated for 14 cycles of operation before it was removed in April 2013 and shipped to MP Machinery & Testing, LLC for opening and testing of the Charpy V-notch surveillance specimens. Evaluation of the fluence environment was conducted by TransWare Enterprises, Inc. Final evaluation of the Charpy test data and irradiated material properties and compilation of this report were performed by EPRI. The Charpy V-notch surveillance materials were tested per ASTM E185-82, and the information and the associated evaluations provided in this report have been performed in accordance with the requirements of 10CFR50 Appendix B [5].

This report compares the irradiated material properties of surveillance plate heat C2557-1 and surveillance weld heat 5P6214B to their baseline (e.g., unirradiated) properties. The observed embrittlement (as characterized by the shift in the Charpy energy curve 30 ft-lb (41J) index temperature or ΔT_{30}) is compared to that predicted by U.S. Nuclear Regulatory Commission (U.S. NRC) Regulatory Guide 1.99, Rev. 2 [6]. Other BWRVIP ISP reports will integrate the results from the 177° capsule with the results from the Perry 3° capsule (withdrawn in 1996), the SSP A, B, and C capsules (withdrawn in 2003), the SSP D capsule (withdrawn in 1996), and the SSP E and F capsules (withdrawn in 2000) for a broader characterization of embrittlement behavior.

1.1 Implementation Requirements

The results documented in this report will be utilized by the BWRVIP ISP and by individual utilities to demonstrate compliance with 10CFR50, Appendix H, Reactor Vessel Material Surveillance Program Requirements. Therefore, the implementation requirements of 10CFR50, Appendix H govern and the implementation requirements of Nuclear Energy Institute (NEI) 03-08, Guideline for the Management of Materials Issues [7], are not applicable.

Section 2: Materials and Test Specimen Description

The General Electric (GE) designed Perry 177° surveillance capsule was removed from the plant and shipped to MP Machinery and Testing, LLC (MPM) for analysis. The capsule was a GE standard single container design, and it held a total of 36 Charpy specimens and 4 dosimetry wires. The 177° capsule is an original plant capsule, and has been irradiated in the plant since initial startup. This is the second surveillance capsule to be removed from Perry and tested. The 3° capsule was tested by GE and the results are reported in [8].

2.1 Dosimeters

The dosimetry wires were located along the ends of the Charpy specimens during irradiation. The surveillance capsule contained a total of 2 iron and 2 copper wires for fluence evaluation. Further details on the exact wire locations during the irradiation are provided in the capsule opening discussion given in Section 2.3. A detailed discussion of the radiometric analysis of the capsule dosimetry wires is provided in Appendix A.

2.2 Test Materials

The 177° Perry capsule Charpy V-notch specimen inventory, material descriptions, unirradiated (baseline) Charpy impact data, and previously measured capsule data are summarized in this section of the report.

2.2.1 Capsule Loading Inventory

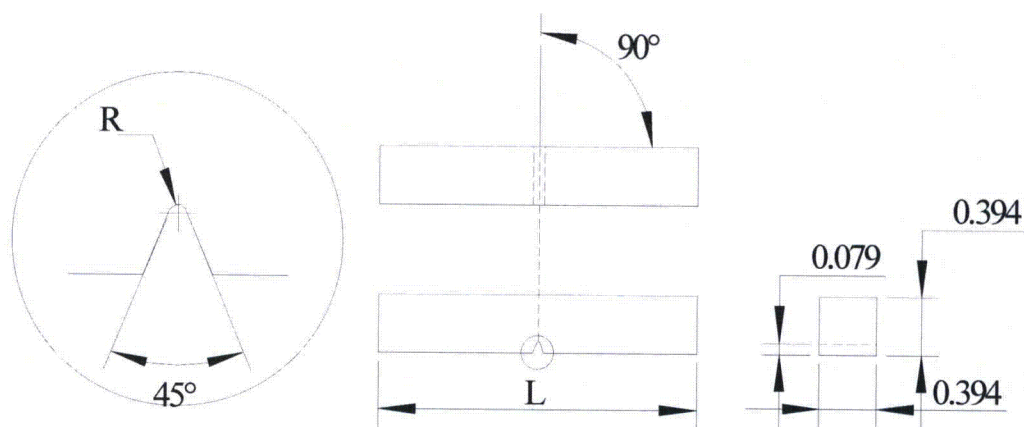
The Perry 177° surveillance capsule inventory is provided in Table 2-1. All of the capsule specimens, which include Charpy specimens and dosimeters, were recovered from the capsule basket. Testing was performed on the 36 Charpy specimens, and the dosimetry wires were counted and weighed to determine specific activities. The broken Charpy specimen halves have been added to long-term archive storage for future use in miniature mechanical behavior specimen testing, chemistry analysis, and microstructural studies.

A drawing of the Charpy test specimen is shown in Figure 2-1 for reference. Photographs of the capsule are given in Figures 2-2 and 2-3. The markings on

the outside of the capsule, including the reactor code and the capsule code were recorded and verified.

Table 2-1
Perry 177° Surveillance Capsule Specimen Inventory

Number of Charpy Specimens			Number of Flux Wires		
Base	Weld	HAZ	Fe	Cu	Ni
12	12	12	2	2	0



ASTM E23 permissible variations shall be as follows:

Notch length to edge:	90 ± 2 degrees
Adjacent sides shall be at:	90 degrees ± 10 minutes
Cross-sectional dimensions:	± 0.003 inches
Length of specimen (L):	2.165 (+0.0, -0.100) inches
Centering of notch (L/2):	± 0.039 inches
Angle of notch:	± 1 degree
Radius of notch:	0.010 ± 0.001 inches
Notch depth:	± 0.001 inches
Finish requirements:	63 μ-inch on notched surface and opposite face; 4 μ-inch elsewhere

Figure 2-1
Drawing Showing the Charpy Test Specimen Geometry and ASTM E23 Permissible Variations

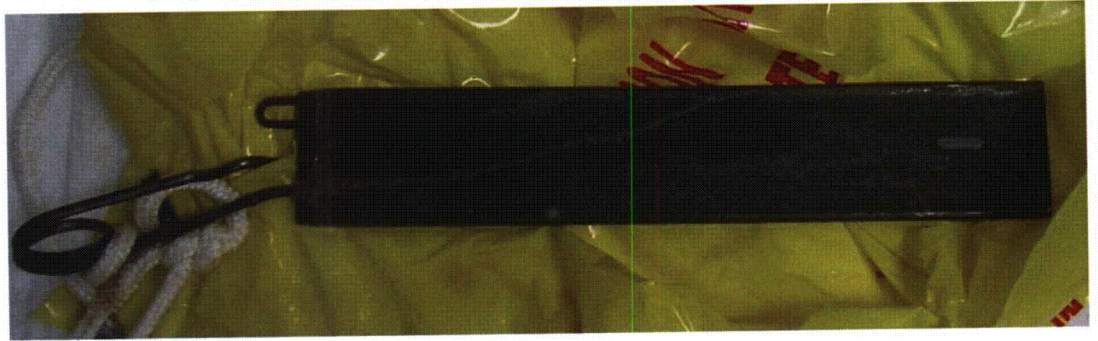


*Figure 2-2
Photograph of the 177° Perry Capsule (top) and a Magnified View of the External
Identification Markings (bottom)*

The Side which Faced the Core in the Plant is Facing Up. The GE Identification Code, "GE131C8981G001/Reactor No. 70", was Engraved Near the Hook.



Figure 2-3
Photograph of the Inside of the 177 Degree Perry Capsule Showing the Dosimetry Location During the Irradiation

2.2.2 Material Description

The Perry Unit 1 plant is a GE BWR/6 design. The pressure vessel construction was performed by CBI Nuclear (CBIN) Company. The pressure vessel plate materials are ASME SA533, Grade B, Class 1 low alloy steel. The surveillance base metal specimens were machined from plate heat number C2557-1 in the transverse-longitudinal orientation (TL). The test plates removed for the surveillance program received the same heat treatment as the vessel including the post-weld heat treatment for 50 hours at 1150 °F +25/-50 °F. Unirradiated baseline data are available for this material and for the weld, but not for the HAZ material. All of the base metal specimens were stamped on the ends with the GE fabrication code listed on the Perry Unit 1 drawings.

The weld and HAZ Charpy surveillance specimens were made by welding together two pieces of the surveillance test plate heat C2557-1. The Reference 8 report states that the weld procedure used for the surveillance specimens was the same as that used for the welds in the beltline region. The welding records from CBIN show the surveillance weld to be a submerged arc weld with heat

5P6214B, Linde 124 flux, and lot 0331. The welded test plates were given a stress relief heat treatment at 1150 °F +25/-50 °F to simulate the pressure vessel fabrication conditions. The base metal orientation for the weld and HAZ specimens is transverse.

2.2.3 Chemical Composition

Table 2-2 details the best estimate average chemistry values for plate heat C2557-1 surveillance material. Chemical compositions are presented in weight percent. If there are multiple measurements on a single specimen, those are first averaged to yield a single value for that specimen, and then the different specimens are averaged to determine the heat best estimate.

Table 2-2

Best Estimate Chemistry of Available Data Sets for Plate Heat C2557-1

Cu (wt%)	Ni (wt%)	P (wt%)	S (wt%)	Si (wt%)	Specimen ID	Source
0.052	0.63	0.011	—	0.25	28983	Reference 8
0.054	0.65	0.014	—	0.26	28984	
0.05	0.61	0.015	—	0.22	28985	
0.06	0.61	0.010	—	0.27	Baseline CMTR	Reference 8
0.05	0.63	0.013	—	0.25	← Best Estimate Average	

Table 2-3 details the best estimate average chemistry values for the weld heat 5P6214B surveillance material. Chemical compositions are presented in weight percent. If there are multiple measurements on a single specimen, those are first averaged to yield a single value for that specimen, and then the different specimens are averaged to determine the heat best estimate.

Table 2-3

Best Estimate Chemistry of Available Data Sets for Weld Heat 5P6214B

Cu (wt%)	Ni (wt%)	P (wt%)	S (wt%)	Si (wt%)	Specimen ID	Source
0.024	0.89	0.013	—	0.46	28971	Reference 8
0.027	0.97	0.014	—	0.50	28972	
0.031	0.97	0.015	—	0.45	28973	
0.027	0.94	0.014	—	0.47	← Best Estimate Average	

2.2.4 CVN Baseline Properties

Tables 2-4 and 2-5 contain the unirradiated Charpy data for the C2557-1 surveillance plate material in the TL and LT orientations, respectively. Tables 2-6 and 2-7 contain the unirradiated Charpy data for the Perry 5P6214B

surveillance weld material and the Supplemental Surveillance Program (SSP) 5P6214B surveillance weld material, respectively.

Table 2-4

Unirradiated Transverse Charpy V-Notch Impact Test Results for Surveillance Base Metal (Heat C2557-1) Specimens from the Perry Surveillance Program

Base Unirradiated: Heat C2557-1, Transverse							
Specimen ID	Test Temperature		Impact Energy		Lateral Expansion		Percent Shear (%)
	°F	(°C)	ft-lb	(J)	mils	(mm)	
31	-50.0	(-45.6)	9.00	(12.20)	9.0	(0.23)	1.0
32	-50.0	(-45.6)	6.00	(8.13)	10.0	(0.25)	1.0
33	-50.0	(-45.6)	11.00	(14.91)	8.0	(0.20)	1.0
28	-20.0	(-28.9)	19.00	(25.76)	11.0	(0.28)	10.0
29	-20.0	(-28.9)	23.00	(31.18)	17.0	(0.43)	10.0
30	-20.0	(-28.9)	13.00	(17.63)	18.0	(0.46)	10.0
25	0.0	(-17.8)	23.00	(31.18)	17.0	(0.43)	20.0
26	0.0	(-17.8)	20.00	(27.12)	23.0	(0.58)	20.0
27	0.0	(-17.8)	18.00	(24.40)	22.0	(0.56)	20.0
1	40.0	(4.4)	32.00	(43.39)	31.0	(0.79)	30.0
2	40.0	(4.4)	32.00	(43.39)	34.0	(0.86)	30.0
3	40.0	(4.4)	36.00	(48.81)	28.0	(0.71)	30.0
10	40.0	(4.4)	44.00	(59.66)	48.0	(1.22)	40.0
11	40.0	(4.4)	51.00	(69.15)	39.0	(0.99)	40.0
12	40.0	(4.4)	40.00	(54.23)	40.0	(1.02)	40.0
22	40.0	(4.4)	40.00	(54.23)	36.0	(0.91)	30.0
23	40.0	(4.4)	46.00	(62.37)	36.0	(0.91)	30.0
24	40.0	(4.4)	40.00	(54.23)	41.0	(1.04)	30.0
4	60.0	(15.6)	40.00	(54.23)	38.0	(0.97)	40.0
5	60.0	(15.6)	46.00	(62.37)	38.0	(0.97)	40.0
6	60.0	(15.6)	44.00	(59.66)	40.0	(1.02)	40.0
13	60.0	(15.6)	54.00	(73.21)	63.0	(1.60)	60.0
14	60.0	(15.6)	64.00	(86.77)	53.0	(1.35)	60.0
15	60.0	(15.6)	76.00	(103.04)	46.0	(1.17)	60.0
7	70.0	(21.1)	52.00	(70.50)	42.0	(1.07)	40.0
8	70.0	(21.1)	50.00	(67.79)	46.0	(1.17)	40.0
9	70.0	(21.1)	52.00	(70.50)	42.0	(1.07)	40.0
19	70.0	(21.1)	60.00	(81.35)	50.0	(1.27)	50.0
20	70.0	(21.1)	62.00	(84.06)	52.0	(1.32)	50.0
21	70.0	(21.1)	58.00	(78.64)	53.0	(1.35)	50.0
16	212.0	(100.0)	86.00	(116.60)	74.0	(1.88)	99.0
17	212.0	(100.0)	84.00	(113.89)	72.0	(1.83)	99.0
18	212.0	(100.0)	87.00	(117.95)	74.0	(1.88)	99.0

Table 2-5

Unirradiated Longitudinal Charpy V-Notch Impact Test Results for Surveillance Base Metal (Heat C2557-1) Specimens from the Perry Surveillance Program

Base Unirradiated: Heat C2557-1, Longitudinal							
Specimen ID	Test Temperature		Impact Energy		Lateral Expansion		Percent Shear (%)
	°F	(°C)	ft-lb	(J)	mils	(mm)	
1	40.0	(4.4)	50.00	(67.79)	47.0	(1.19)	40.0
2	40.0	(4.4)	53.00	(71.86)	44.0	(1.12)	40.0
3	40.0	(4.4)	50.00	(67.79)	44.0	(1.12)	40.0
4	40.0	(4.4)	64.00	(86.77)	54.0	(1.37)	50.0
5	40.0	(4.4)	54.00	(73.21)	54.0	(1.37)	50.0
6	40.0	(4.4)	65.00	(88.13)	43.0	(1.09)	50.0

Table 2-6

Unirradiated Charpy V-Notch Impact Test Results for Surveillance Weld Metal (Heat 5P6214B, Lot 0331, Linde 124 Flux, Single Wire) Specimens from the Perry Surveillance Program

Weld Unirradiated: Heat 5P6214B, Lot 0331, Linde 124 Flux, Single Wire							
Specimen ID	Test Temperature		Impact Energy		Lateral Expansion		Percent Shear (%)
	°F	(°C)	ft-lb	(J)	mils	(mm)	
1	-70.0	(-56.7)	22.00	(29.83)	17.0	(0.43)	2.0
2	-70.0	(-56.7)	13.00	(17.63)	10.0	(0.25)	2.0
3	-70.0	(-56.7)	11.00	(14.91)	9.0	(0.23)	2.0
4	-50.0	(-45.6)	42.00	(56.94)	34.0	(0.86)	15.0
5	-50.0	(-45.6)	13.00	(17.63)	11.0	(0.28)	5.0
6	-50.0	(-45.6)	34.00	(46.10)	26.0	(0.66)	10.0
7	10.0	(-12.2)	56.00	(75.92)	45.0	(1.14)	25.0
8	10.0	(-12.2)	50.00	(67.79)	41.0	(1.04)	20.0
9	10.0	(-12.2)	54.00	(73.21)	46.0	(1.17)	30.0
10	40.0	(4.4)	76.00	(103.04)	66.0	(1.68)	75.0
11	40.0	(4.4)	66.00	(89.48)	52.0	(1.32)	45.0
12	100.0	(37.8)	87.00	(117.95)	70.0	(1.78)	95.0
13	100.0	(37.8)	89.00	(120.67)	64.0	(1.63)	90.0
14	120.0	(48.9)	96.00	(130.16)	68.0	(1.73)	100.0
15	120.0	(48.9)	90.00	(122.02)	61.0	(1.55)	100.0
16	120.0	(48.9)	88.00	(119.31)	71.0	(1.80)	100.0

Table 2-7

Unirradiated Charpy V-Notch Impact Test Results for Surveillance Weld Metal (Heat 5P6214B, Lot 0331, Linde 124 Flux) Specimens from the Supplemental Surveillance Program (SSP)

Weld Unirradiated: Heat 5P6214B, Lot 0331, Linde 124 Flux							
Specimen ID	Test Temperature		Impact Energy		Lateral Expansion		Percent Shear
	°F	(°C)	ft-lb	(J)	mils	(mm)	(%)
1	-80.0	(-62.2)	7.5	(10.17)	1.5	(0.04)	7.0
2	-60.0	(-51.1)	19.00	(25.76)	13.5	(0.34)	23.0
3	-40.0	(-40.0)	17.00	(23.05)	10.5	(0.27)	25.0
4	-20.0	(-28.9)	31.50	(42.71)	22.5	(0.57)	34.0
5	-20.0	(-28.9)	45.00	(61.01)	26.5	(0.67)	43.0
6	0.0	(-17.8)	41.50	(56.27)	26.0	(0.66)	31.0
7	20.0	(-6.7)	61.00	(82.70)	44.0	(1.12)	56.0
8	20.0	(-6.7)	56.00	(75.93)	39.0	(0.99)	57.0
9	40.0	(4.4)	68.00	(92.20)	51.0	(1.30)	72.0
10	60.0	(15.6)	76.00	(103.04)	54.5	(1.38)	85.0
11	80.0	(26.7)	82.00	(111.18)	61.5	(1.56)	84.0
12	100.0	(37.8)	86.00	(116.60)	69.0	(1.75)	99.0
13	180.0	(82.2)	93.00	(126.09)	79.0	(2.01)	100.0
14	300.0	(148.9)	93.00	(126.09)	73.5	(1.87)	100.0
15	400.0	(204.4)	94.00	(127.45)	70.0	(1.78)	100.0

The baseline test data were fit to a hyperbolic tangent curve using the computer program CVGRAPH [9]. Figures 2-4 and 2-5 show the fitted Charpy energy data curves for the unirradiated plate and weld, respectively. For the 5P6214B weld heat, the curve in Figure 2-5 is fit to the combined unirradiated data from Tables 2-6 and 2-7. Table 2-8 summarizes the baseline (unirradiated) Charpy V-notch properties (index temperatures) of plate heat C2557-1 and weld heat 5P6214B. In this table and throughout this report, T_{30} is the 30 ft-lb (41 J) transition temperature; T_{50} is the 50 ft-lb (68 J) transition temperature; $T_{35\text{mil}}$ is the 35 mil (0.89 mm) lateral expansion temperature; and USE is the average energy absorption at full shear fracture appearance.

Table 2-8
Baseline CVN Properties

Material Identity	Material	T₃₀ °F (°C)	T₅₀ °F (°C)	T_{35mil} °F (°C)	Upper Shelf Energy (USE) ft-lb (J)
C2557-1 (TL orientation)	Perry Surveillance Plate	18.5 (-7.5)	56.8 (13.8)	35.6 (2.0)	85.7 (116.2)
5P6214B	Perry Surveillance Weld	-33.2 (-36.2)	2.7 (-16.3)	-2.9 (-19.4)	90.9 (123.2)

2.2.5 Tanh Curve Fits of CVN Test Data for Plate Heat C2557-1

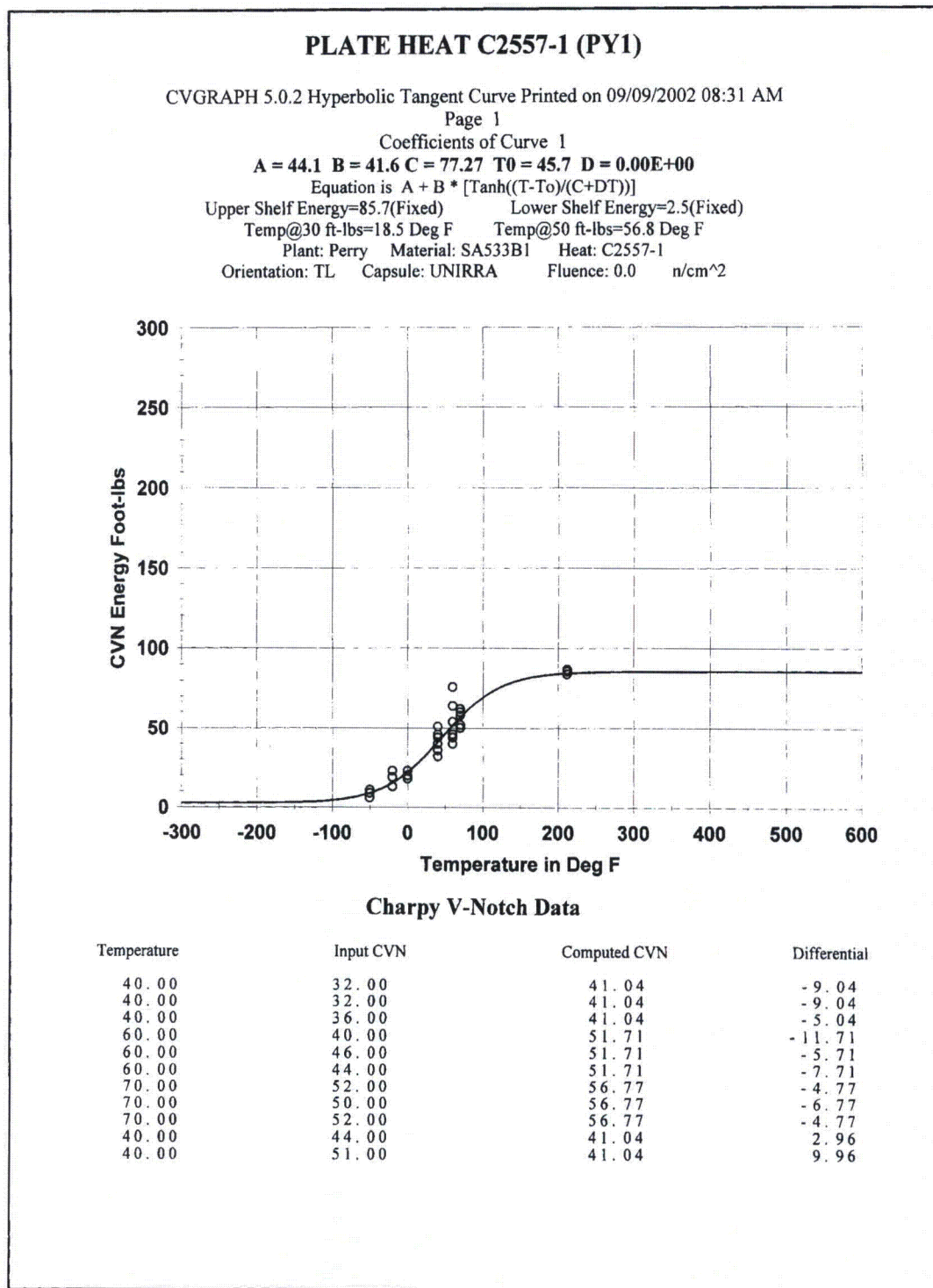


Figure 2-4
Charpy Energy Data for Plate Heat C2557-1 (TL) Unirradiated

PLATE HEAT C2557-1 (PY1)

Page 2

Plant: Perry Material: SA533B1 Heat: C2557-1
 Orientation: TL Capsule: UNIRRA Fluence: 0.0 n/cm²

Charpy V-Notch Data

Temperature	Input CVN	Computed CVN	Differential
40.00	40.00	41.04	-1.04
60.00	54.00	51.71	2.29
60.00	64.00	51.71	12.29
60.00	76.00	51.71	24.29
212.00	86.00	84.59	1.41
212.00	84.00	84.59	-.59
212.00	87.00	84.59	2.41
70.00	60.00	56.77	3.23
70.00	62.00	56.77	5.23
70.00	58.00	56.77	1.23
40.00	40.00	41.04	-1.04
40.00	46.00	41.04	4.96
40.00	40.00	41.04	-1.04
.00	23.00	22.01	.99
.00	20.00	22.01	-2.01
.00	18.00	22.01	-4.01
-20.00	19.00	15.34	3.66
-20.00	23.00	15.34	7.66
-20.00	13.00	15.34	-2.34
-50.00	9.00	8.95	.05
-50.00	6.00	8.95	-2.95
-50.00	11.00	8.95	2.05

Correlation Coefficient = .949

Figure 2-4 (continued)
 Charpy Energy Data for Plate Heat C2557-1 (TL) Unirradiated

2.2.6 Tanh Curve Fits of CVN Test Data for Weld Heat 5P6214B

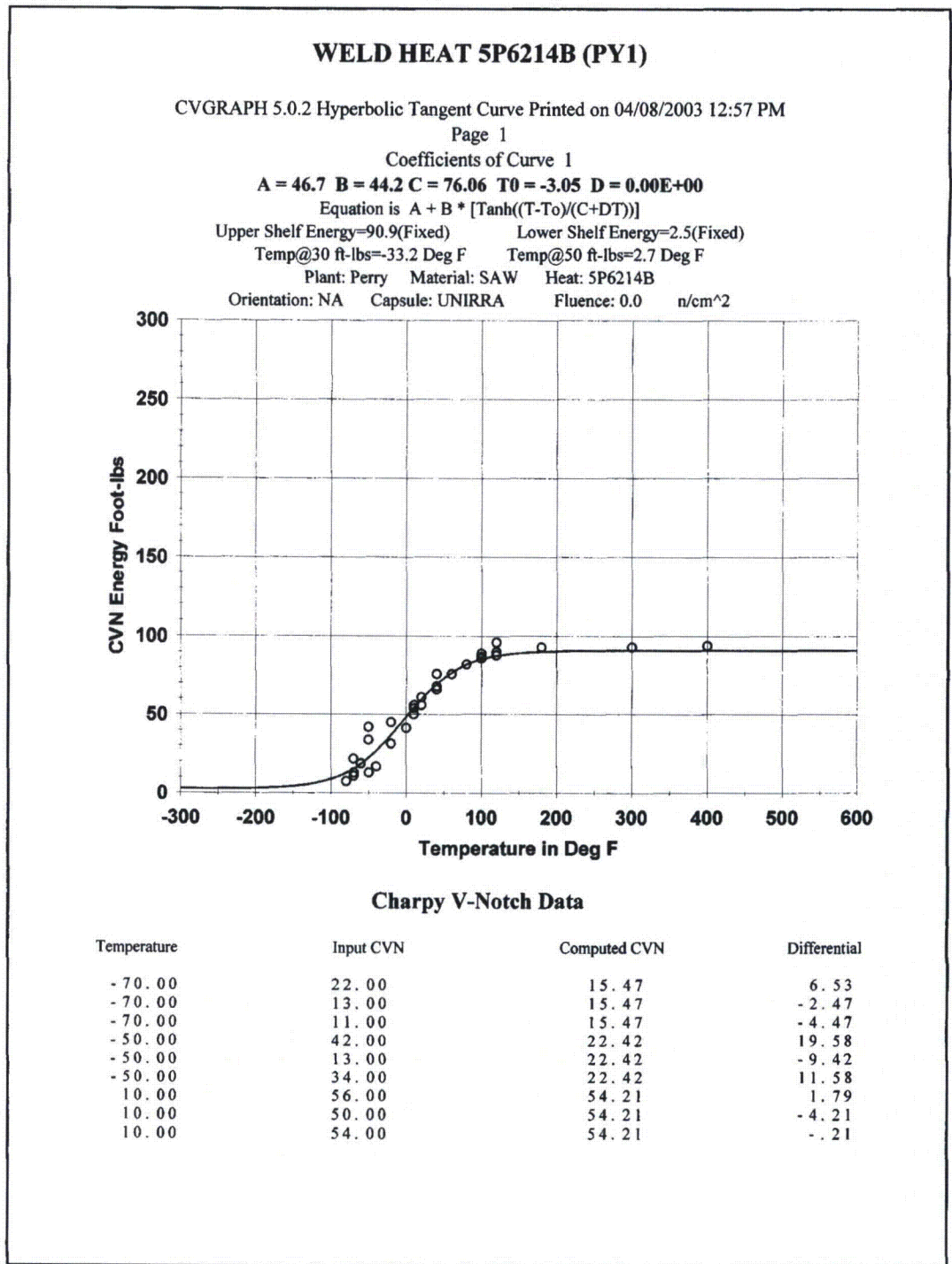


Figure 2-5
Charpy Energy Data for Weld Heat 5P6214B Unirradiated

WELD HEAT 5P6214B (PY1)

Page 2

Plant: Perry Material: SAW Heat: 5P6214B
Orientation: NA Capsule: UNIRRA Fluence: 0.0 n/cm²

Charpy V-Notch Data

Temperature	Input CVN	Computed CVN	Differential
40.00	76.00	69.35	6.65
40.00	66.00	69.35	-3.35
100.00	87.00	85.38	1.62
100.00	89.00	85.38	3.62
120.00	96.00	87.56	8.44
120.00	90.00	87.56	2.44
120.00	88.00	87.56	.44
-80.00	7.50	12.82	-5.32
-60.00	19.00	18.66	.34
-40.00	17.00	26.77	-9.77
-20.00	31.50	37.01	-5.51
-20.00	45.00	37.01	7.99
.00	41.50	48.47	-6.97
20.00	61.00	59.70	1.30
20.00	56.00	59.70	-3.70
40.00	68.00	69.35	-1.35
60.00	76.00	76.75	-.75
80.00	82.00	81.95	.05
100.00	86.00	85.38	.62
180.00	93.00	90.19	2.81
300.00	93.00	90.87	2.13
400.00	94.00	90.90	3.10

Correlation Coefficient = .979

Table 2-5 (continued)
Charpy Energy Data for Weld Heat 5P6214B Unirradiated

2.3 Capsule Opening

The 177° surveillance capsule was opened on October 21, 2013. As shown in Figures 2-2 and 2-3, the 177° capsule consisted of a single container. The outside of the capsule had identification markings and codes which could be clearly read. The capsule container was engraved with the following markings:

Reactor Code: 70

Capsule Code: GE131C8981G001

As expected, the Reactor Code is consistent with the markings observed on the 3° capsule described in Reference 8.

Attention was paid to the location of the Charpy specimens and the dosimetry wire locations during disassembly of the capsule. The dosimetry wire location along the ends of the Charpy specimens is shown in Figure 2-3. Referring to the figure, the 12 base metal specimens were installed at the top of the capsule, the 12 weld specimens were in the middle, and the 12 HAZ specimens were installed in the bottom of the capsule. The dosimetry wires and Charpy specimens were placed in individually marked containers for positive identification throughout the work. The base metal specimens were marked on the ends with the designation "BP1", the weld specimens were marked "WP2", and the HAZ specimens were marked "HP3". MPM assigned a sequential numbering to uniquely identify each specimen and to maintain traceability to the position within the capsule

Section 3: Neutron Fluence Calculation

The 177° capsule was irradiated in Perry for 14 cycles of operation. It was placed in the reactor's 177° capsule holder prior to cycle 1 and was removed following cycle 14 for a total irradiation period of 20.0 effective full power years (EFPY). The surveillance capsule included copper and iron flux wire dosimetry specimens.

Evaluation of the surveillance capsule specimens requires knowledge of the neutron irradiation environment. The neutron flux density, neutron energy spectrum, and neutron fluence are required at the surveillance capsule location. The NRC has established guidelines in Regulatory Guide 1.190 [10] for determining best estimate values of flux, energy spectrum, and fluence for RPV damage assessments using particle transport methods. These guidelines are not specifically intended for use in surveillance capsule evaluations; however, the guidelines provide suitable guidance to support the development of accurate neutron transport analysis models for surveillance capsule evaluations.

This report documents the application of the modeling and analysis guidelines provided in [10] to determine the surveillance capsule accumulated irradiation and capsule specimen neutron fluence of the Perry 177° ISP capsule flux wires. Additionally, the accumulated irradiation for the 3° capsule flux wires, removed at the end of cycles (EOC) 1 and 5, were determined. The fast neutron fluence ($E > 1.0$ MeV) was also calculated for the 3° capsules at the time of removal and for the 177° capsule at the time of removal. The fluence and activation values presented in this report were calculated using the RAMA Fluence Methodology [11] (hereinafter referred to as "RAMA"). The specific activities predicted by RAMA are compared to the activity measurements reported in Appendix A.

RAMA has been developed for the Electric Power Research Institute, Inc. (EPRI) and the BWRVIP for the purpose of calculating neutron fluence in Boiling Water Reactor (BWR) components. As prescribed in Regulatory Guide 1.190, RAMA has been benchmarked against industry standard benchmarks for both pressurized water reactor (PWR) and BWR designs. In addition, RAMA has been compared with several plant-specific dosimetry measurements and reported fluences from several commercial operating reactors. The results of the benchmarks and comparisons to measurements show that RAMA accurately predicts specimen activities, RPV fluence, and vessel internal component fluence in all light water reactor types. Under funding from EPRI and the BWRVIP, the RAMA methodology has been reviewed by the U. S. NRC and subsequently given generic approval for determining fast neutron fluence in BWR pressure

vessels [12] and vessel internal components that include the core shroud and top guide [13].

3.1 Description of the Reactor System

This section provides an overview of the reactor design and operating data inputs that were used to develop the Perry reactor fluence model. All reactor design and operating data inputs used to develop the model were plant-specific and were provided by Perry. The inputs for the fluence geometry model were developed from design and as-built drawings for the reactor pressure vessel, vessel internals, fuel assemblies, and containment regions. The reactor operating data inputs were developed from core simulator data that provided a historical accounting of how the reactor operated for cycles 1 through 14.

3.1.1 Reactor System Mechanical Design

Perry is a General Electric BWR/6 class reactor with a core loading of 748 fuel assemblies. Perry began commercial operation in 1986 with a design rated power of 3579 MWt. A power uprate was achieved in operating cycle 8 raising the thermal power output to 3758 MWt. At the time of this fluence analysis, Perry had completed 14 cycles of operation.

Figure 3-1 illustrates the basic planar configuration of the Perry reactor at an axial elevation near the reactor core mid-plane. All of the radial regions of the reactor that are required for fluence projections are shown. Beginning at the center of the reactor and projecting outward, the regions include: the core region, including control rod locations and fuel assembly locations (fuel locations are shown only for the 0° to 90° quadrant); core reflector region (bypass water); central shroud wall; downcomer water region including the jet pumps; reactor pressure vessel (RPV) wall; cavity region between the RPV wall and insulation; insulation; cavity region between the insulation and biological shield; and biological shield (concrete wall).

The mechanical design inputs that were used to construct the Perry fluence geometry model included as-built and nominal design dimensional data. As-built data for the reactor components and regions of the reactor system is always preferred when constructing plant-specific models; however, as-built data is not always available. In these situations, nominal design information is used.

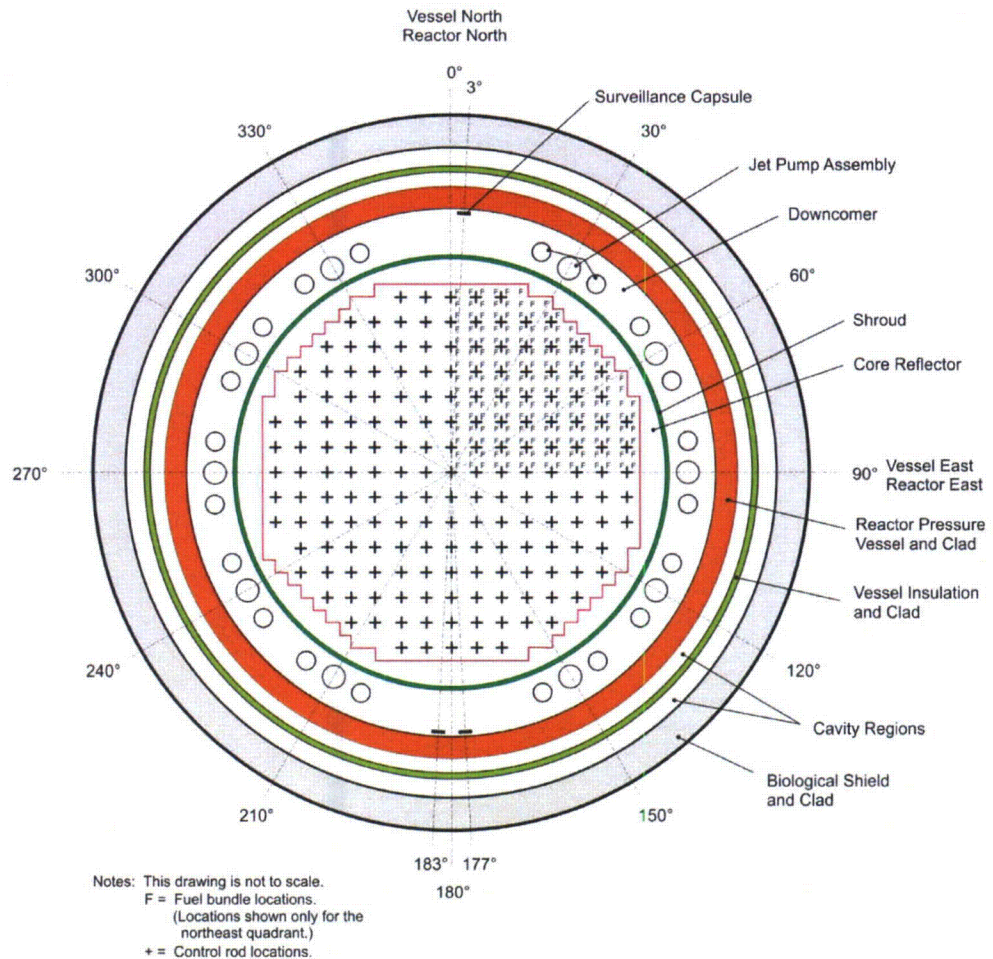


Figure 3-1
Planar View of Perry at the Core Mid-plane Elevation

For the Perry fluence model, the predominant dimensional information used to construct the fluence model was nominal design data. As-built data was used for the following dimension:

- Capsule container mounting pads

Another important component of the fluence analysis is the accurate description of the surveillance capsules in the reactor. It is shown in Figure 3-1 that three surveillance capsules were initially installed in the Perry reactor. The capsules were attached radially to the inside surface of the RPV (looking outward from the core region) at the 3°, 177°, and 183° azimuths. Surveillance capsules are used to monitor the radiation accumulated in the reactor over a period of time. The importance of surveillance capsules in fluence analyses is that they contain flux wires that are irradiated during reactor operation. When a capsule is removed from the reactor, the irradiated flux wires are evaluated to obtain activity measurements. These measurements are used to validate the fluence model. Three sets of flux wires have been removed from the Perry reactor and analyzed.

(See Section 3.3, which presents a comparison of the calculated-to-measured capsule results.)

3.1.2 Reactor System Material Compositions

Each region of the reactor is comprised of materials that include reactor fuel, steel, water, insulation, concrete, and air. Accurate material information is essential for the fluence evaluation as the material compositions determine the scattering and absorption of neutrons throughout the reactor system and, thus, affect the determination of neutron fluence in the reactor components.

Table 3-1 provides a summary of the materials for the various components and regions of the Perry reactor. The material attributes for the steel, insulation, concrete, and air compositions (i.e. material densities and isotopic concentrations) are assumed to remain constant for the operating life of the reactor. The attributes of the fuel compositions in the reactor core region change continuously during an operating cycle due to changes in power level, fuel burnup, control rod movements, and changing moderator density levels (voids). Because of the dynamics of the fuel attributes with reactor operation, several state-point data sets are used to describe the operating states of the reactor for each operating cycle. The number of data sets used in this analysis is presented in Section 3.1.3.3.

Table 3-1
Summary of Material Compositions by Region for Perry

Region	Material Composition
Control Rods and Guide Tubes	Stainless Steel
Core Support Plate	Stainless Steel
Fuel Support Piece	Stainless Steel
Fuel Assembly Lower Tie Plate	Stainless Steel, Zircaloy, Inconel
Reactor Core	^{235}U , ^{238}U , ^{239}Pu , ^{240}Pu , ^{241}Pu , ^{242}Pu , O_{fuel} , Zircaloy
Reactor Coolant / Moderator	Water
Core Reflector	Water
Fuel Assembly Upper Tie Plate	Stainless Steel, Zircaloy, Inconel
Top Guide	Stainless Steel
Core Spray Sparger Pipes	Stainless Steel
Core Spray Sparger Flow Areas	Water
Shroud	Stainless Steel
Downcomer Region	Water
Jet Pump Riser and Mixer Flow Areas	Water
Jet Pump Riser and Mixer Metal	Stainless Steel
Jet Pump Riser Brace and Pad	Stainless Steel
Surveillance Capsule Containers	Stainless Steel
Surveillance Capsule Specimens	Carbon Steel
Reactor Pressure Vessel Clad	Stainless Steel
Reactor Pressure Vessel Wall	Carbon Steel
Cavity Regions	Air (Nitrogen)
Insulation Clad	Stainless Steel
Insulation	Aluminum
Biological Shield Clad	Carbon Steel
Biological Shield Wall	Reinforced Concrete

3.1.3 Reactor Operating Data Inputs

An accurate evaluation of reactor vessel and component fluence requires an accurate accounting of the reactor's operating history. The primary reactor operating parameters that affect the determination of fast neutron fluence in light

water reactors include reactor power levels, core power distributions, coolant water density distributions, and fuel material (isotopic) distributions.

3.1.3.1 Core Loading

It is common in BWRs that more than one fuel assembly design may be loaded in the reactor core in any given operating cycle. For fluence evaluations, it is important to account for the fuel assembly designs that are loaded in the core in order to accurately represent the neutron source distribution at the core boundaries (i.e. peripheral fuel locations and the top and bottom fuel elevations).

Three different fuel assembly mechanical designs were loaded in the Perry reactor during the period included in this evaluation. Table 3-2 provides a summary of the fuel mechanical designs loaded in the reactor core for each evaluated operating cycle. The cycle core loading provided by Perry was used to identify the fuel assembly designs in each cycle and their location in the core loading inventory. (Note that fuel loadings for cycles 4 and 8 were divided into two individual periods, identified as 4A, 4B, 8A, and 8B.) For each cycle, appropriate fuel assembly models were used to build the reactor core region of the Perry RAMA fluence model.

3.1.3.2 Power History Data

Reactor power history is the measure of reactor power levels and core exposure on a continual or periodic basis. For this fluence evaluation, the power history for the Perry reactor was developed from power history inputs provided by Perry. The power history data showed that Perry started commercial operation with a design rated thermal power of 3579 MWt. A power uprate was implemented during cycle 8 raising the thermal power output to 3758 MWt.

The power history data for Perry included daily power levels for all cycles. This data was used to calculate the capsule and vessel fluence. Periods of reactor shutdown due to refueling outages and other events were also accounted for in the model. The power history data was verified by comparing the calculated energy production in effective full power years with power production records provided by Perry. Table 3-3 lists the accumulated EFPY at the end of each cycle for this fluence evaluation.

Table 3-2
Summary of Perry Core Loading Inventory

Cycle	8x8 Designs			9x9 Designs	10x10 Designs		Dominant Peripheral Design
	GE6	GE8	GE10	GE11	GE12	GE14	
1	748						GE 8x8
2	476	272					GE 8x8
3	204	544					GE 8x8
4A	5	539	204				GE 8x8
4B	10	534	204				GE 8x8
5		320	428				GE 8x8
6		40	472	236			GE 8x8
7			260	236	252		GE 8x8
8A			36	181	531		GE 9x9
8B			36	183	529		GE 9x9
9					444	304	GE 10x10
10					164	584	GE 10x10
11						748	GE 10x10
12						748	GE 10x10
13						748	GE 10x10
14						748	GE 10x10

3.1.3.3 Reactor State-Point Data

Core simulator data was provided by Perry to characterize the historical operating conditions of Perry for cycles 1 through 14 and cycle projections. The data calculated with core simulator codes represents the best-available information about the reactor core's operating history over the reactor's operating life. In this analysis, the detailed core simulator data was processed by TransWare to generate state-point data files for input to the RAMA fluence model. The state-point files included three-dimensional data arrays that described core power distributions, fuel exposure distributions, fuel materials (isotopics), and coolant water densities.

A separate neutron transport calculation was performed for each of the state points tallied in Table 3-3. The calculated neutron flux for each state point was combined with the appropriate power history data described in Section 3.1.3.2 in order to provide an accurate accounting of the fast neutron fluence for the reactor pressure vessel and surveillance capsule.

3.1.3.4 Beginning of Operation through Cycle 14 State Points

A total of 245 state points were used to represent the operating history for the first 14 operating cycles of Perry. These state points were selected from hundreds of exposure points that were calculated with the core simulator code. The hundreds of exposure points were evaluated and grouped into a fewer number of exposure ranges in order to reduce the number of transport calculations required to perform the fluence evaluation. Several criteria were used in the determination of the exposure ranges, including evaluations of core thermal powers, core flows, core power profiles, and control rod patterns. In determining exposure ranges, it is assumed that there will be at least one exposure step in that range that would accurately represent the average operating conditions of the reactor over that range. This single exposure step is then referred to as the "state point". Table 3-3 shows the number of state points used for each cycle in this fluence evaluation.

Table 3-3
State-point Data for Each Cycle of Perry

Cycle Number	Number of State Points	Rated Thermal Power ¹ (MWt)	Accumulated Effective Full Power Years (EFPY)
1	23	3579	1.1
2	20	3579	2.1
3	13	3579	3.2
4A	8	3579	3.7
4B	10	3579	4.2
5	18	3579	5.5
6	19	3579	6.8
7	17	3579	8.2
8A	9	3579	9.2
8B	9	3758	9.9
9	19	3758	11.6
10	12	3758	13.2
11	21	3758	15.0
12	12	3758	16.6
13	16	3758	18.4
14	19	3758	20.0

¹ The rated thermal power is listed for each cycle. The actual power levels were used for the individual state-point calculations for cycles 1-14.

3.2 Calculation Methodology

This section provides an overview of the Perry fluence model that was developed with the RAMA Fluence Methodology software [11]. The RAMA fluence model for Perry is a plant-specific model that was constructed from the design inputs described in Section 3.1.

3.2.1 Description of the RAMA Fluence Methodology

The RAMA Fluence Methodology (RAMA) is a system of computer codes, a data library, and an uncertainty methodology that determines best-estimate fluence in light water reactor pressure vessels and vessel components. The primary codes that comprise the RAMA methodology include model builder codes, a particle transport code, and a fluence calculator code. The data library contains nuclear cross sections and response functions that are needed for each of the codes. The uncertainty methodology is used to determine the uncertainty and bias in the best-estimate fluence calculated by the software.

The primary inputs for RAMA are mechanical design parameters and reactor operating history data. The mechanical design inputs are obtained from plant-specific design drawings, which include as-built measurements when available. The reactor operating history data is obtained from reactor core simulator codes, system heat balance calculations, daily operating logs, and cycle summary reports that describe the operating conditions of the reactor over its operating lifetime. The primary outputs from RAMA calculations are neutron flux, neutron fluence, dosimetry activation, and an uncertainty evaluation.

The model builder codes consist of geometry and material processor codes that generate input for the particle transport code. The geometry model builder code uses mechanical design inputs and meshing specifications to generate three-dimensional geometry models of the reactor. The material processor code uses reactor operating data inputs to process fuel materials, structural materials, and water densities that are consistent with the geometry meshing generated by the geometry model builder code.

The particle transport code performs three-dimensional neutron flux calculations using a deterministic, multigroup, particle transport theory method with anisotropic scattering. The primary inputs prepared by the user for the transport code include the geometry and material data generated by the model builder codes and numerical integration and convergence parameters for the iterative transport calculation. The transport solver is coupled with a general geometry modeling capability based on combinatorial geometry techniques. The coupling of general geometry with a deterministic transport solver provides a flexible, accurate, and efficient tool for calculating neutron flux in light water reactor pressure vessels and vessel components. The primary output from the transport code is the neutron flux in multigroup form.

The fluence calculator code determines fluence and activation in the reactor pressure vessel and vessel components over specified periods of reactor operation.

The primary inputs to the fluence calculator include the multigroup neutron flux from the transport code, response functions for the various materials in the reactor, reactor power levels for the operating periods of interest, the specification of which components to evaluate, and the energy ranges of interest for evaluating neutron fluence. The fluence calculator includes treatments for isotopic production and decay that are required to calculate specific activities for irradiated materials. The reactor operating history is generally represented with several reactor state points that represent the various power levels and core power shapes generated by the reactor over the life of the plant. These detailed state points are combined with the daily reactor power levels to produce accurate estimates of the fluence and activations accumulated in the plant.

The uncertainty methodology provides an assessment of the overall accuracy of the RAMA Fluence Methodology. Variances in the dimensional data, reactor operating data, dosimetry measurement data, and nuclear data are evaluated to determine if there is a statistically significant bias in the calculated results that might affect the determination of the best-estimate fluence for the reactor. The plant-specific results are also weighted with comparative results from experimental benchmarks and other plant analyses and analytical uncertainties pertaining to the methodology to determine if the plant-specific model under evaluation is statistically acceptable as defined in Regulatory Guide 1.190.

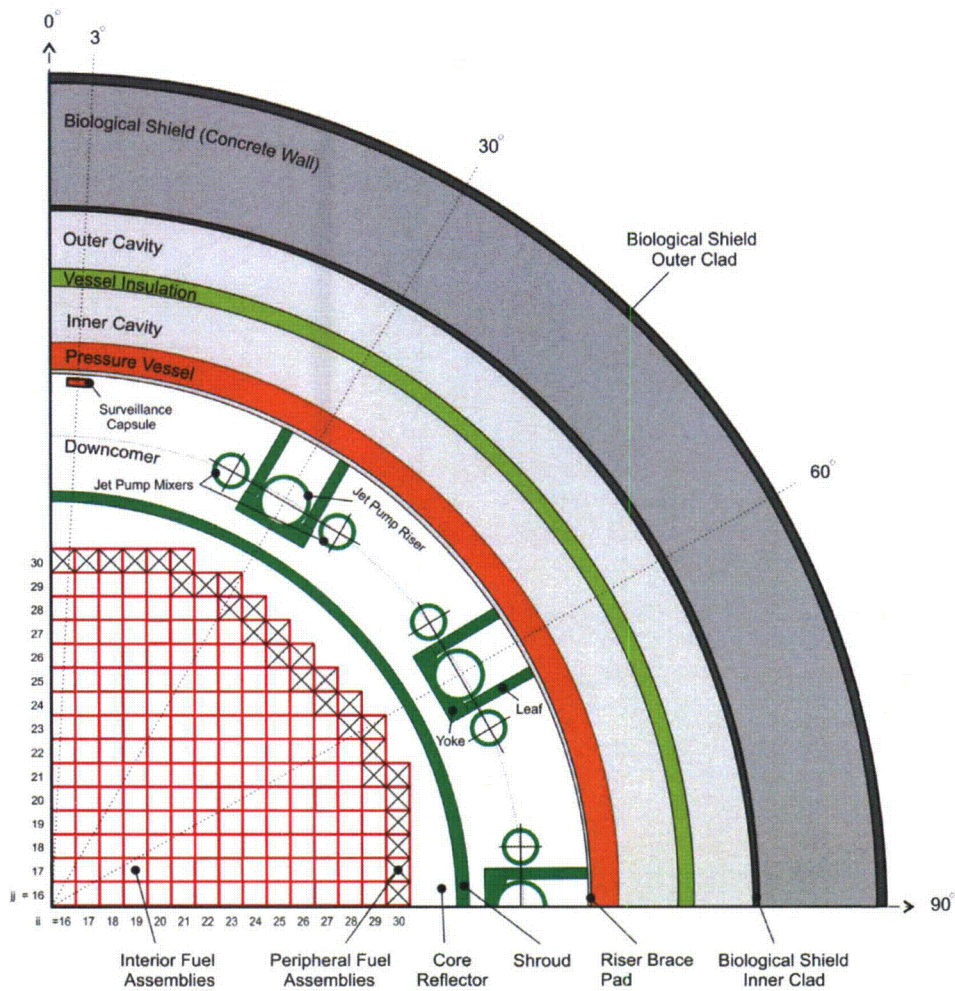
The RAMA nuclear data library contains atomic mass data, nuclear cross-section data, and response functions that are needed in the material processing, transport, fluence, and reaction rate calculations. The cross-section data and response functions are based on the BUGLE-96 nuclear data library [14] and the VITAMIN-B6 data library [15].

The RAMA Fluence Methodology is described in the Theory Manual [16]. The general procedures for using the methodology are presented in the Procedures Manual [17].

3.2.2 RAMA Geometry Model for the Perry Reactor

Section 3.1 describes the design inputs that were provided by FirstEnergy Nuclear Operating Company for the Perry reactor fluence evaluation. These design inputs were used to develop a plant-specific, three-dimensional computer model of the Perry reactor with the RAMA Fluence Methodology.

Figures 3-2 and 3-3 provide general illustrations of the primary components, structures and regions developed for the Perry fluence model. Figure 3-2 shows the planar configuration of the reactor model at an elevation corresponding to the reactor core mid-plane elevation. Figure 3-3 shows an axial configuration of the reactor model. Note that the figures are not drawn to scale. They are intended only to provide a perspective for the layout of the model, and specifically how the various components, structures, and regions lie relative to the reactor core region (i.e., the neutron source).



Notes: This drawing is not to scale.
 * In quadrant symmetry, this capsule represents the 3°, 177° and 183° capsules

Figure 3-2
 Planar View of the Perry RAMA Quadrant Model at the Core Mid-plane Elevation

Because the figures are intended only to provide a general overview of the model, they do not include illustrations of the geometry meshing developed for the model. To provide such detail is beyond the scope of this document.

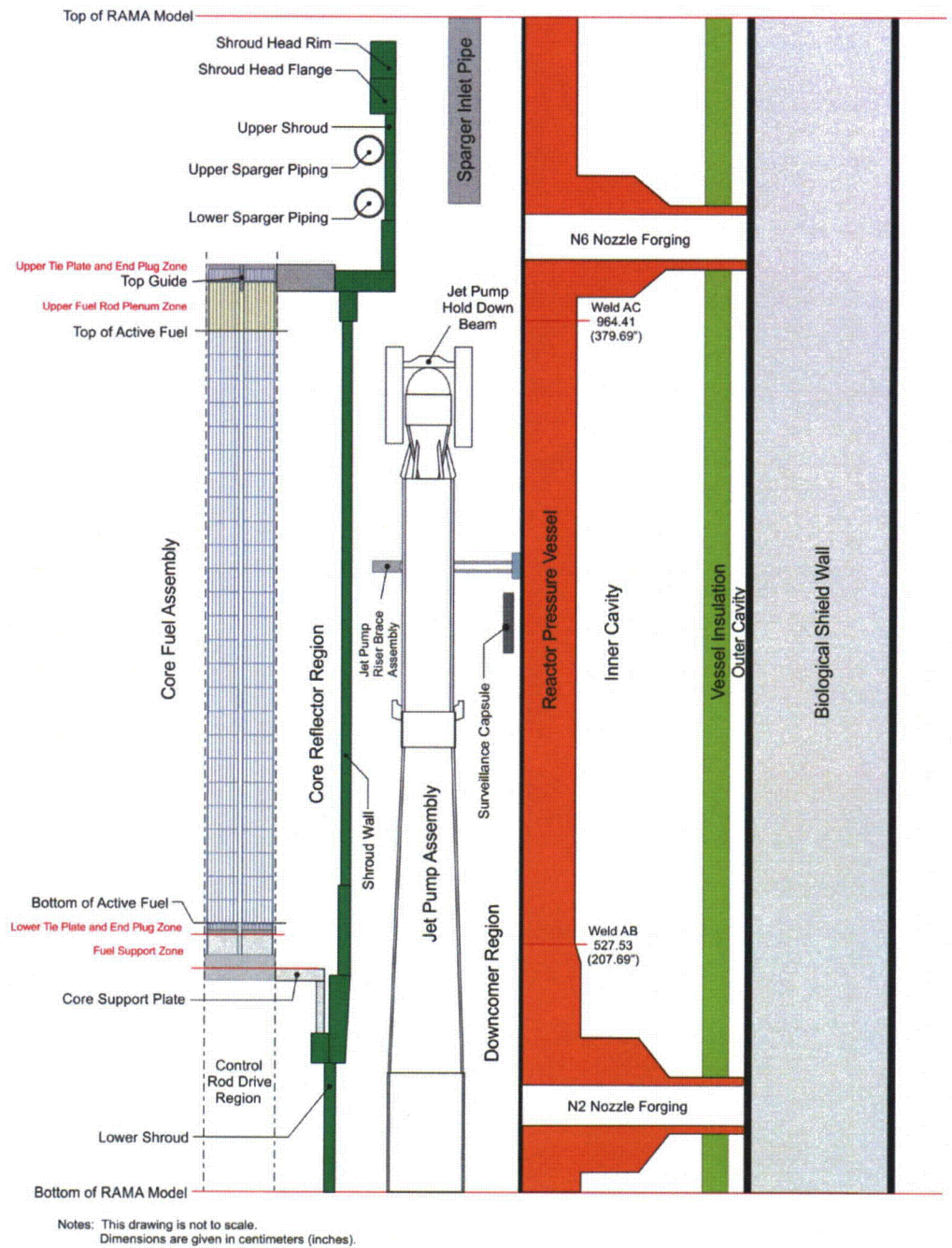


Figure 3-3
Axial View of the Perry RAMA Model

The following subsections provide an overview of the computer models that were developed for the various components, structures, and coolant flow regions of the Perry reactor.

3.2.2.1 Geometry Model

RAMA uses a generalized three-dimensional geometry modeling system that is based on a combinatorial geometry technique, which is mapped to a Cartesian coordinate system. In this analysis, an axial plane of the reactor model is defined by the (x,y) coordinates of the modeling system and the axial elevation at which a plane exists is defined along a perpendicular z-axis of the modeling system. Thus, any point in the reactor model can be addressed by specifying the (x,y,z) coordinates for that point.

Figure 3-1 illustrates a planar cross-section view of the Perry reactor design at an axial elevation corresponding to the reactor core mid-plane elevation. It is shown for this one elevation that the reactor design is a complex geometry composed of various combinations of rectangular, cylindrical, and wedge-shaped bodies. When the reactor is viewed in three dimensions, the varying heights of the different components, structures, and regions create additional geometry modeling complexities. An accurate representation of these geometrical complexities in a predictive computer model is essential for calculating accurate, best-estimate fluence in the reactor pressure vessel, the vessel internals, and the surrounding structures.

Figures 3-2 and 3-3 provide general illustrations of the planar and axial geometry complexities that are represented in the Perry fluence model. For comparison purposes, the planar view illustrated in Figure 3-2 corresponds to the same core mid-plane elevation illustrated in Figure 3-1. The computer model for Perry assumes azimuthal quadrant symmetry in the planar dimension.

Figure 3-2 illustrates the quadrant geometry that was modeled in this analysis. In terms of the modeling coordinate system, the "northeast" quadrant of the geometry is represented in the model. The 0° azimuth, which has a "north" designation, corresponds to the 0° azimuth referenced in the plan drawings for the reactor pressure vessel. Degrees are incremented clockwise. Thus, the 90° azimuth is designated as the "east" direction. All other components, structures, and regions have been appropriately mirror reflected or rotated to this quadrant based upon their relationship to the pressure vessel orientation to ensure that the fluence is appropriately calculated relative to the neutron source (i.e., the core region). Although symmetry is a modeling consideration, the results presented in this report for the different components and structures are given at their correct azimuths in the plant.

Figure 3-3 illustrates the axial configuration of the primary components, structures, and regions in the fluence model. For discussion purposes, the same components, structures, and regions shown in the planar view of Figure 3-2 are also illustrated in Figure 3-3. Figure 3-3 shows that the axial height of the fluence model spans from a lower elevation just below the jet pump riser inlet to above the core shroud head flange. This axial height covers all areas of the reactor pressure vessel that are expected to exceed a fluence threshold of $1.0\text{E}+17$ n/cm² at 54 EFPY.

As previously noted, Figures 3-2 and 3-3 are not drawn precisely to scale. They are intended only to provide a perspective of how the various components, structures, and regions of the reactor are positioned relative to the reactor core region (i.e., the neutron source) and each other. The following subsections provide details on the modeling of individual components, structures, and regions. Please refer to the figures for visual orientation of the components and regions described in the following subsections.

3.2.2.2 Reactor Core and Core Reflector Models

The reactor core contains the nuclear fuel that is the source of the neutrons that irradiate all components and structures of the reactor. The core is surrounded by a shroud structure that serves to channel the reactor coolant through the core region during reactor operation. The region between the core and the core shroud is the core reflector, and it contains coolant. The reactor core geometry is rectangular in design and is modeled with rectangular elements to preserve its shape in the analysis. The core reflector region interfaces with the rectangular shape of the core region and the curved shape of the core shroud. It is, therefore, modeled using a combination of rectangular and cylindrical elements.

The core region is centered in the reactor pressure vessel and is characterized in the analysis with two fundamental fuel zones: interior fuel assemblies and peripheral fuel assemblies. The peripheral fuel assemblies are the primary contributors to the neutron source in the fluence calculation. Because these assemblies are loaded at the core edge where neutron leakage from the core is greatest, there is a sharp power gradient across these assemblies that requires consideration. To account for the power gradient, the peripheral fuel assemblies are sub-meshed with additional rectangular elements that preserve the pin-wise details of the fuel assembly geometry and power distribution. The interior fuel assemblies make a lesser contribution to the reactor fluence and are, therefore, modeled in various homogenized forms in accordance with their contributions to the reactor fluence. For computational efficiency, homogenization treatments are used in the interior core region primarily to reduce the number of mesh regions that must be solved in the transport calculation. The meshing configuration for each fuel assembly location in the core region is determined by parametric studies to ensure an accurate estimate of fluence throughout all regions of the reactor system.

Each fuel assembly design, whether loaded in the interior or peripheral locations in the core, is represented with four axial material zones: the lower tie plate/end plug zone, the fuel zone, the fuel upper plenum zone, and the upper tie plate/end plug zone. The structural materials in the top and bottom nozzles for each unique assembly design are represented in the model to address the shielding effects that these materials have on the components above and below the core region. The fuel zone contains the nuclear fuel and structural materials for the fuel assemblies. The materials for each fuel assembly are unique during reactor operation and are incorporated into the model using reactor operating data from core simulator codes. The upper plenum region captures fission gases during reactor operation.

From an isotopic standpoint, the core is modeled using quadrant symmetry. For the 3° and 177° capsule evaluations, as well as the peak RPV fluence calculations, the northeast fuel quadrant was used. It was noted during the evaluation that some of the cycles experienced abnormal power tilts across the core due to power suppression control rod maneuvers. It was determined that these abnormalities would not significantly impact the capsule activation analyses or lead factor calculations, but could contribute to higher standard deviations in the activation results.

3.2.2.3 Core Shroud Model

The core shroud is a canister-like structure that contains the reactor core and channels the reactor coolant and steam produced by the core into the steam separators. Axially the shroud extends from the lower shroud wall to the top of the shroud head rim in the model. The core shroud is cylindrical in design and is modeled with pipe elements.

3.2.2.4 Downcomer Region Model

The downcomer region lies between the core shroud and the reactor pressure vessel. It is basically cylindrical in design, but with some geometrical complexities created by the presence of jet pumps and surveillance capsules in the region. The majority of the downcomer region is modeled with pipe segments. The areas of the downcomer containing the jet pumps and specimen capsules are modeled with the appropriate geometry elements to represent their design features and to preserve their radial, azimuthal, and axial placement in the downcomer region. These structures are described further in the following subsections.

3.2.2.5 Jet Pump Model

There are ten jet pump assemblies in the downcomer region of Perry, which provide the main recirculation flow for the core. The jet pumps are modeled at azimuths 30°, 60°, and 90° in the downcomer region. When symmetry is applied to the model, the 30° location represents the jet pump assemblies that are positioned azimuthally at 30°, 150°, 210°, and 330°; the 60° location represents those at 60°, 120°, 240°, and 300°; and the 90° location represents the jet pump assemblies at 90° and 270°. Note that there are no jet pumps present at the 0° and 180° azimuths of the reactor.

The jet pump model includes representations for the riser, mixer, and diffuser pipes; nozzles; rams head; hold down beams and brackets; and riser brace yoke, leafs, and pad. The jet pump assembly design is modeled using cylindrical pipe elements for the jet pump riser and mixer pipes. The riser pipe is correctly situated between the mixer pipes. The riser brace assembly model includes two leaf structures that attach to the yoke and circumferential pad.

3.2.2.6 Surveillance Capsule Model

Section 3.1 describes the three surveillance capsules installed in the Perry reactor. The surveillance capsules are installed near the inner surface of the pressure vessel wall. The surveillance capsules are rectangular in design. Because of this shape, the capsules are not easily implemented in the otherwise cylindrical elements of the downcomer region model. With reference to Figure 3-1, it is observed that the capsules are of small dimensions in the planar geometry and they reside a long distance (view factor) from the core region. Based on these factors, the otherwise rectangular shape of the surveillance capsules can be reasonably approximated in the model with arc elements. The surveillance capsule model also includes a representation for the downcomer water that surrounds the capsule on all sides.

The surveillance capsules are correctly modeled behind the jet pump riser pipes at the 3° azimuth. When symmetry is applied to the model, the 3° location represents the capsules installed at 3° and 177°.

The surveillance capsules are modeled at their correct axial position and height relative to the core region.

3.2.2.7 Reactor Pressure Vessel Model

The reactor pressure vessel and vessel cladding lie outside the downcomer region and each is cylindrical in design. Both are modeled with pipe elements. The cladding-pressure vessel interface is a key location for RPV fluence calculations and is preserved in the model. This interface defines the inside surface (OT) for the pressure vessel base metal where the RPV fluence is calculated. Perry has cladding only on the inside surface of the pressure vessel wall. Representations of the forgings for the recirculation inlet (N2) and RHR/LPCI (N6) nozzles are also included in the model out to the biological shield radius.

3.2.2.8 Vessel Insulation Model

The vessel insulation lies in the cavity region outside the pressure vessel wall. The insulation is cylindrical in design and follows the contour of the pressure vessel wall. It is modeled with pipe elements.

3.2.2.9 Inner and Outer Cavity Models

The cavity region lies between the pressure vessel and biological shield structures. As previously described, the vessel insulation lies in the cavity region; thus creating two cavity regions. The inner cavity region lies between the vessel and the insulation. The outer cavity region lies between the vessel insulation and biological shield cladding. The boundaries of the cavity regions follow the contours of the pressure vessel, vessel insulation, and biological shield. The cavity regions are essentially cylindrical in design and are modeled with pipe segments.

3.2.2.10 Biological Shield Model

The biological shield (concrete) defines the outer most region of the fluence model. The biological shield is basically cylindrical in design and is modeled with pipe segments. There is cladding on the inside and outside surfaces of the biological shield.

3.2.2.11 Above-Core Component Models

Figure 3-3 includes illustrations of other components and regions that lie above the reactor core region. The predominant above-core components represented in the model include the top guide and core spray spargers.

3.2.2.11.1 Top Guide Model

The top guide component lies above the core region. The top guide is appropriately modeled by including representations for the vertical fuel assembly parts and top guide plates. The upper fuel assembly parts that extend into the top guide region are modeled in three axial segments: the fuel rod plenum, fuel rod upper end plugs, and fuel assembly upper tie plate. The fuel assembly parts and top guide plates are modeled with rectangular elements.

3.2.2.11.2 Core Spray Sparger Model

The core spray spargers include upper and lower sparger pipes and a vertical inlet pipe. The core spray spargers are appropriately represented as torus structures in the model. The sparger pipes reside inside the upper shroud wall above the top guide. The spargers are modeled as pipe-like structures and include a representation of steam inside the pipes.

3.2.2.12 Below-Core Component Models

Figure 3-3 includes illustrations of other components and regions that lie below the reactor core region. The fuel support piece, core support plate, and core inlet regions appropriately include a representation of the cruciform control rod below the core region. The lower fuel assembly parts include representations for the fuel rod lower end plugs, lower tie plate, and nose piece. The below-core components include representations for the fuel support elements and control rod guide mechanisms. These are modeled using various combinations of cylindrical pipe elements and rectangular bodies to represent the control rod blades themselves.

3.2.2.13 Summary of the Geometry Modeling Approach

To summarize the reactor modeling process, there are several key features of the RAMA code system that allow the reactor design to be accurately represented for RPV and capsule fluence evaluations. Following is a summary of some of the key features of the model.

- Rectangular, cylindrical, and wedge bodies are mixed in the model in order to provide an accurate geometrical representation of the components and regions in the reactor.
- The reactor core geometry is modeled with rectangular bodies to represent its actual shape in the reactor. The fuel assemblies in the core region are also sub-meshed with additional rectangular bodies to represent the pin cell regions in the assemblies.
- A combination of rectangular and cylindrical bodies is used to describe the transition parts between the rectangular core region and the cylindrical outer core regions.
- Cylindrical and wedge bodies are used to model the components and regions that extend outward from the core region (core shroud, downcomer, RPV, etc.).
- The surveillance capsules are modeled at their correct radial, azimuthal, and elevational positions in the downcomer region.
- The above-core region includes accurate representations of the top guide and core spray spargers.
- The below-core region includes appropriate representations for the fuel support piece, core support plate, core inlet regions, cruciform control rods, and control rod drives.
- The biological shield is appropriately represented as a cylindrical body.

3.2.3 RAMA Calculation Parameters

The RAMA transport code uses a three-dimensional deterministic transport method to calculate the neutron flux. The accuracy of the transport method is based on a numerical integration technique that uses ray-tracing to characterize the geometry, anisotropy treatments to determine the directional flow of particles, and convergence parameters to determine the overall accuracy of the flux solution between iterates. The code allows the user to specify values for each of these parameters.

The primary input parameters that control the ray-tracing calculation are the distance between parallel rays in the planar and axial dimensions, the depth that a particle is tracked when a reflective boundary is encountered, and the number of equally spaced angles in polar coordinates for tracking the particles. Plant-specific values are determined for each of the parameters. The RAMA transport calculation employs a treatment for anisotropy that is based on a Legendre expansion of the scattering cross sections. By default, the RAMA transport calculation uses the maximum order of expansion that is available for each nuclide in the RAMA nuclear data library. For the actinide and zirconium nuclides, a P_5 expansion of the scattering cross sections is used. For all other nuclides, a P_7 expansion of the scattering cross sections is used.

The overall accuracy of the neutron flux calculation is determined using an iterative technique to converge the flux iterations. The convergence criterion used

in the evaluation was determined by parametric study to provide an asymptotic solution for this model.

3.2.4 RAMA Neutron Source Calculation

RAMA calculates a unique neutron source distribution for each transport calculation using the input relative power density factors for the fuel region and data from the RAMA nuclear data library. The source distribution changes with fuel burnup; thus, the source is determined using core-specific three-dimensional burnup distributions at frequent intervals throughout a cycle. For the fluence model, the peripheral fuel assemblies are modeled to preserve the power gradient at the core edge that is formed from the pin-wise source distributions in these fuel assemblies.

3.2.5 RAMA Fission Spectra

RAMA calculates a weighted fission spectrum for each transport calculation that is based on the relative contributions of ^{235}U , ^{238}U , ^{239}Pu , ^{240}Pu , ^{241}Pu , and ^{242}Pu isotopes. The fission spectra for these isotopes are derived from the BUGLE-96 nuclear data library.

3.3 Surveillance Capsule Activation and Fluence Results

This section documents the fluence and activation results for the Perry reactor. The activation results also form the basis for the validation and qualification of the application of the RAMA Fluence Methodology to the Perry reactor in accordance with the requirements of Reg. Guide 1.190. Reg. Guide 1.190 requires fluence calculational methods to be validated by comparison with measurements from operating reactor dosimetry for the specific plant being analyzed or for reactors of similar design. The acceptance criteria provided in Reg. Guide 1.190 is that the comparison to measurement ratios (C/M) and standard deviation values must be $\leq 20\%$. All of the Perry reactor capsule measurement comparisons to the RAMA predicted values meet the Reg. Guide 1.190 limits. The accuracy of the comparisons is additional confirmation that the RAMA Fluence Methodology provides unbiased fluence estimates for the Perry reactor dosimetry.

Three flux wire activation analyses have been performed for the Perry reactor. Flux wires were removed from the 3° capsule flux wire holder and analyzed at the end of cycle 1 (irradiated for 1.1 EFPY); surveillance capsule flux wires were removed at the end of cycle 5 from the 3° capsule (irradiated for 5.5 EFPY); and surveillance capsule flux wires were removed at the end of cycle 14 from the 177° capsule (irradiated for 20.0 EFPY). Details of the dosimetry specimens and analysis are presented in Section 3.3.1.

Best estimate fast fluence ($E > 1.0$ MeV) was calculated for all of the removed capsules and the 3° capsule flux wire holder. Lead factors are determined and reported for all removed capsules.

3.3.1 Comparison of Predicted Activation to Plant-specific Measurements

The comparison of predicted activation for the Perry cycles 1, 5, and 14 flux wires to measurements is presented in this subsection. Fluence values are also calculated and reported in Section 3.3.2 for each of the capsule flux wires.

3.3.1.1 Cycle 1 3° Flux Wire Holder Activation Analysis

Iron flux wires were irradiated in the Perry surveillance capsule flux wire holder at the 3° azimuth during the first cycle of operation. The wires were removed after being irradiated for a total of 1.1 EFPY. Activation measurements were performed following irradiation for the following reaction [18]: $^{54}\text{Fe} (n,p) ^{54}\text{Mn}$. The precise location of the individual wires within the surveillance capsule flux wire holder is not known, therefore, the activation calculations were performed at the center of the holder.

Table 3-4 provides a comparison of the RAMA calculated specific activities and the measured specific activities for the flux wire specimens. The cycle 1 total flux wire average calculated-to-measured (C/M) value is 1.01 with a standard deviation of ± 0.00 .

Table 3-4

Comparison of Specific Activities for Perry Cycle 1 3° Flux Wire Holder Wires (C/M)

Flux Wires	Measured Activity (dps/g)	Calculated Activity (dps/g)	Ratio of Calculated to Measured Activities	Standard Deviation
Iron				
Iron A	8.69E+04	8.82E+04	1.01	
Iron B	8.70E+04	8.82E+04	1.01	—
Iron C	8.69E+04	8.82E+04	1.01	—
Average	8.69E+04	8.82E+04	1.01	0.00
Total Flux Wire Average	---	---	1.01	0.00

3.3.1.2 Cycle 5 3° Surveillance Capsule Activation Analysis

Copper and iron flux wires were irradiated in the Perry surveillance capsule at the 3° azimuth during the first 5 cycles of operation. The wires were removed after being irradiated for a total of 5.5 EFPY. Activation measurements were performed following irradiation for the following reactions [12]: $^{63}\text{Cu} (n,\alpha) ^{60}\text{Co}$ and $^{54}\text{Fe} (n,p) ^{54}\text{Mn}$. The precise location of the individual wires within the surveillance capsule is not known, therefore, the activation calculations were performed at the center of the capsule.

Table 3-5 provides a comparison of the RAMA calculated specific activities and the measured specific activities for the surveillance capsule flux wire specimens. The cycle 5 capsule total flux wire average C/M value is 1.00 with a standard deviation of ± 0.08 .

Table 3-5
Comparison of Specific Activities for Perry Cycle 5 3° Surveillance Capsule Flux Wires (C/M)

Flux Wires	Measured Activity (dps/g)	Calculated Activity (dps/g)	Ratio of Calculated to Measured Activities	Standard Deviation
Iron				
Average	1.46E+05	1.56E+05	1.07	
Copper				
Average	1.55E+04	1.44E+04	0.93	
Total Flux Wire Average	---	---	1.00	0.08

3.3.1.3 Cycle 14 177° Surveillance Capsule Activation Analysis

Copper and iron flux wires were irradiated in the Perry surveillance capsule at the 177° azimuth during the first 14 cycles of operation. The wires were removed after being irradiated for a total of 20.0 EFPY. Activation measurements were performed following irradiation for the following reactions [3]: $^{63}\text{Cu} (n,\alpha) ^{60}\text{Co}$ and $^{54}\text{Fe} (n,p) ^{54}\text{Mn}$. The precise location of the individual wires within the surveillance capsule was not known at the time the activation calculations were performed, therefore, the calculations were performed at the center of the capsule.

Table 3-6 provides a comparison of the RAMA calculated specific activities and the measured specific activities for the surveillance capsule flux wire specimens. The cycle 14 capsule total flux wire average C/M value is 1.03 with a standard deviation of ± 0.14 .

Table 3-6

Comparison of Specific Activities for Perry Cycle 14 177° Surveillance Capsule Flux Wires (C/M)

Flux Wires	Measured Activity (dps/g)	Calculated Activity (dps/g)	Ratio of Calculated to Measured Activities	Standard Deviation
Iron				
Fe-1	132.55	148.58	1.12	—
Fe-2	127.30	148.58	1.17	—
Average	129.93	148.58	1.14	0.03
Copper				
Cu-1	25.21	23.00	0.91	—
Cu-2	25.22	23.00	0.91	—
Average	25.22	23.00	0.91	0.00
Total Flux Wire Average	---	---	1.03	0.14

3.3.1.4 Surveillance Capsule Activation Analysis Summary

Table 3-7 presents a summary of the total average calculated-to-measured result of specific activities for all Perry flux wires. Combining all flux wires (copper and iron), the total average C/M is 1.01 with a standard deviation of ±0.09.

Table 3-7

Comparison of Activities for Perry Flux Wires

Dosimeter	Number of Measurements	Ratio of Calculated to Measured Activities	Standard Deviation
3° Flux Wire (EOC 1)	3	1.01	0.00
3° Capsule (EOC 5)	4	1.00	0.08
177° Capsule (EOC 14)	4	1.03	0.14
Total	11	1.01	0.09

3.3.2 Capsule Peak Fluence Calculations and Lead Factor Determinations

Best estimate fast neutron fluence was calculated for each of the capsules removed from the Perry reactor. Of the three original capsules, two have been removed, one from the 3° location and the other from the 177° location. The

surveillance capsule at the 183° location remains installed in the reactor. The fluence for the capsules is reported at the time of their removal. Additionally, the lead factor for each capsule is calculated by dividing the peak capsule fluence by the respective peak RPV fluence at a given reporting time. The results of these calculations are presented in Table 3-8.

It is observed in Table 3-8 that the lead factors vary between cycles and capsules. In theory, a plant running with a consistent fuel loading pattern and a symmetric power shape will have similar lead factors for all capsules, since the capsules usually reside in symmetric locations.

*Table 3-8
Calculated Capsule Fast Neutron Fluence and Lead Factors for Perry*

Capsule	Time of Removal	EFPY at Removal	Capsule Fluence (E>1.0 MeV, n/cm ²)	RPV Peak Fluence (E>1.0 MeV, n/cm ²)	Lead Factor
3°	EOC 1	1.1 EFPY	5.14E+16	7.51E+16	0.68
3°	EOC 5	5.5 EFPY	3.18E+17	5.19E+17	0.61
177°	EOC 14	20.0 EFPY	1.08E+18	1.82E+18	0.59

3.4 Capsule Fluence Uncertainty Analysis

This section presents the combined uncertainty analysis and bias determination for the Perry capsule fluence evaluation. The combined uncertainty is comprised of the comparison uncertainty factors developed in Section 3.3 and an analytic uncertainty factor developed in this section. When combined, these components provide a basis for determining the overall uncertainty (1σ) and bias in the capsule fluence for this analysis.

The requirements for determining the combined uncertainty and bias for light water reactor fluence evaluations are provided in Regulatory Guide 1.190. The method implemented for determining the combined uncertainty and bias for reactor component fluence is described in the RAMA Theory Manual [16]. Regarding the determination of a bias in the fluence, Regulatory Guide 1.190 provides that an adjustment to the calculated fluence for bias effects is needed if a statistically significant bias exists in the fluence computation.

The results presented in this section show that the combined uncertainty for the Perry capsule fluence evaluation is 10.7% and that no adjustment for bias effects is required to the calculated capsule fluence reported in Section 3.3 of this report.

The following subsections describe the comparison uncertainties determined in Section 3.3, the determination of the analytic uncertainty, and the determination of the overall combined uncertainty and bias for the Perry capsule fluence evaluation.

3.4.1 Comparison Uncertainty

Comparison uncertainty factors are determined by comparing calculated activities with activity measurements. For capsule fluence evaluations, two comparison uncertainty factors are considered: an operating reactor comparison uncertainty factor and a benchmark comparison uncertainty factor. The determination of a comparison uncertainty factor based on measurements involves the combination of two measurement components. One component is the variation in the comparison of the calculated-to-measured (C/M) activity ratio and the other accounts for the uncertainty introduced by the measurement process.

3.4.1.1 Operating Reactor Comparison Uncertainty

The operating reactor, or plant-specific, comparison uncertainty for the Perry reactor is determined by combining the standard deviation for the activity comparisons with the measurement uncertainty for the plant-specific activity measurements.

3.4.1.2 Benchmark Comparison Uncertainty

The benchmark comparison uncertainty used in the Perry uncertainty analysis is based on a set of industry standard simulation benchmark comparisons.

3.4.2 Analytic Uncertainty

The calculational models used for fluence analyses are comprised of numerous analytical parameters that have associated uncertainties in their values. The uncertainty in these parameters needs to be tested for its contribution to the overall fluence uncertainty.

The uncertainty values for the geometry parameters are based upon uncertainties in the dimensional data used to construct the plant geometry model. The uncertainty values for the material parameters are based upon uncertainties in the material densities for the water and nuclear fuel materials and the compositional makeup of typical steel materials.

The uncertainty values for the fission source parameters are based upon uncertainties in the fuel exposure and power factors for the fuel assemblies loaded on the core periphery. The transport method used in the fluence analysis employs a fission source calculation that accounts for the relative contributions of the uranium and plutonium fissile isotopes in the fuel and the relative power density of the fuel in the reactor. Both fission source parameters are derived directly from information calculated by three-dimensional core simulator codes. The uncertainty values for the nuclear cross-section parameters are based upon uncertainties in the number densities for the predominant nuclides that make up the reactor materials.

The uncertainty parameters for the fluence model inputs are based upon geometry meshing and numerical integration parameters used in the neutron flux

transport calculation. The process for determining the geometry meshing and numerical integration parameters involves an exhaustive sensitivity study that is described in the RAMA Procedures Manual [17].

3.4.3 Combined Uncertainty

The combined uncertainty for the capsule fluence evaluation is determined with a weighting function that combines the analytic, plant-specific comparison, and benchmark comparison uncertainty factors developed in Sections 3.4.1 and 3.4.2, above. Table 3-9 shows that the combined uncertainty (1σ) determined for the Perry capsule fluence is 10.7% for energy >1.0 MeV.

Table 3-9 also shows that, in accordance with Regulatory Guide 1.190, no bias term exists and it is not necessary to adjust the RAMA predicted capsule fluence in this analysis for bias effects. It is also demonstrated in Table 3-9 that the combined uncertainty is within the limits prescribed in U. S. NRC Regulatory Guide 1.190 (i.e. $\leq 20\%$).

Table 3-9
Perry Capsule Uncertainty for Energy >1.0 MeV

Uncertainty Term	Value
Combined Uncertainty (1σ)	10.7%
Bias	None ¹

¹ The bias terms are less than their constituent uncertainty values, concluding that no statistically significant bias exists.

Section 4: Charpy Test Data

4.1 Charpy Test Procedure

Charpy impact tests were conducted in accordance with American Society for Testing and Materials (ASTM) Standards E185-82 [3] and E23-02 [19]. The 1982 version of E185 has been reviewed and approved by NRC for surveillance capsule testing applications. This standard references ASTM E23 [19]. The tests were conducted using a Tinius Olsen Testing Machine Company, Inc. Model 84 impact test machine with a 300 ft-lb (406.75 J) energy capacity. The Model 84 is equipped with a dial gage as well as the MPM optical encoder system for accurate absorbed energy measurement. The machine is also equipped with an instrumented striker, so a total of three independent measurements of the absorbed energy were made for every test. In all cases, the optical encoder measured energy was reported as the impact energy. The optical encoder energy is much more accurate than the analog dial. The optical encoder can resolve the energy to within 0.04 ft-lbs (0.054 J), whereas, for the dial, the resolution is around 0.25 ft-lbs (0.34 J). The impact energy was corrected for windage and friction for each test performed. The velocity of the striker at impact was nominally 18 ft/s (5.49 m/s). The MPM encoder system measures the exact impact velocity for every test. Calibration of the machine was verified as specified in ASTM E23, and verification specimens were obtained from the National Institute for Standards and Technology (NIST) and tested in accordance with the standard.

The ASTM E23 procedure for specimen temperature control using an in-situ heating and cooling system was followed. The advantage of using the MPM in-situ heating/cooling technology is that each specimen is thermally conditioned right up to the instant of impact. Thermal losses associated with liquid bath systems, such as those resulting from transfer of a specimen from a liquid bath to the test machine, are completely eliminated. Each specimen was held at the desired test temperature for at least 5 minutes prior to testing, and the fracture process zone temperature was held to within $\pm 1.8^\circ \text{F}$ ($\pm 1^\circ \text{C}$) up to the instant of strike. Precision calibrated tongs were used for specimen centering on the test machine.

Lateral expansion (LE) was determined from measurements made with a lateral expansion gage. The lateral expansion gage was calibrated using precision gage blocks which are traceable to NIST. The percentage of shear fracture area was determined by integrating the ductile and brittle fracture areas using the MPM Digital Optical Comparator (DOC) image analysis system. As shown in Figure

4-1, each fracture surface image is captured, outlined to delineate the brittle area, and outlined to define the outer ductile fracture region. The DOC software then performs a pixel area integration and automatically calculates the shear fracture area. This method for shear area determination is the most accurate method given in ASTM E23, and is far superior to the commonly used photograph comparison method.

The number of Charpy specimens for measurement of the transition region and upper shelf was limited. Therefore, the choice of test temperatures was very important. Prior to testing, the Charpy energy-temperature curve was predicted using embrittlement models and previous data. The first test was then conducted near the middle of the transition region, and test temperature decisions were then made based on the test results. Overall, the goal was to perform two or three tests on the upper shelf, and to use the remaining specimens to characterize the 30 ft-lb (41 J) index. This approach was successful and the transition region and upper shelf energy are well defined.

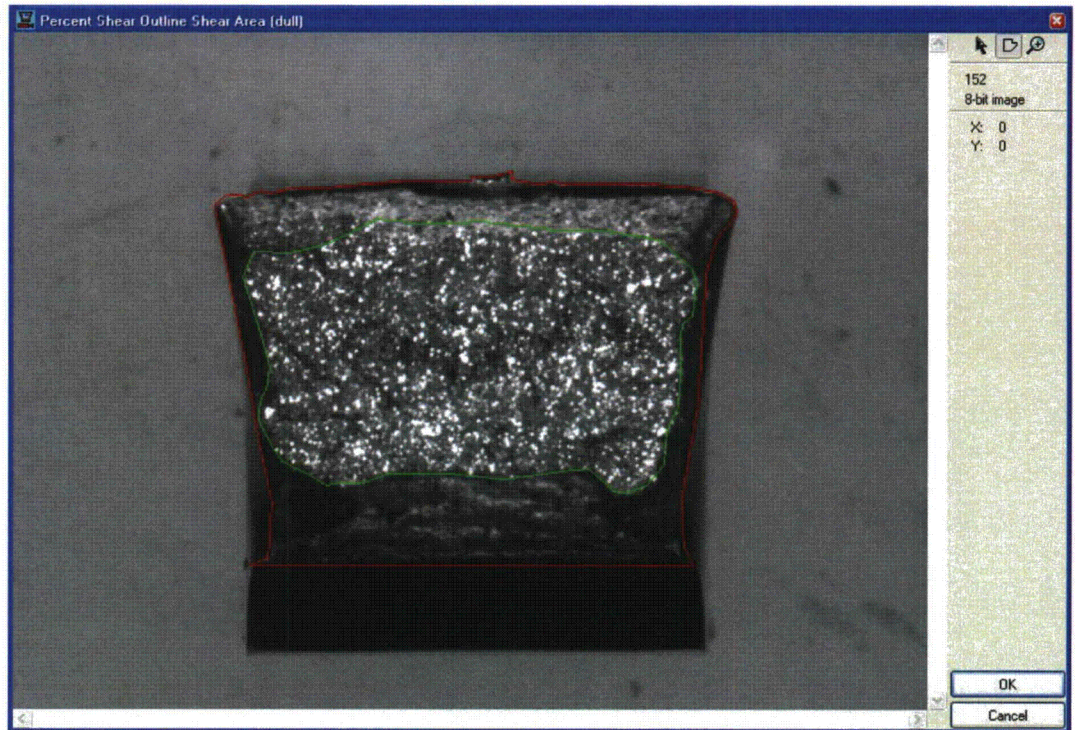


Figure 4-1
Illustration of Digital Optical Comparator Measurement of Shear Fracture Area

First, the Brittle Fracture Area is Outlined (within green line). Next, the Outer Ductile Fracture Area is Outlined (within red line). Finally, the Software Integrates the Areas and Calculates the Percent Shear Fracture Area.

4.2 Charpy Test Data for 177° Capsule

A total of twelve irradiated base, weld, and HAZ metal specimens, respectively, were tested over the transition region temperature range and on the upper shelf. The data are summarized in Tables 2-1 through 2-3. In addition to the energy absorbed by the specimen during impact, the measured lateral expansion values and the percentage shear fracture area for each test specimen are listed in the tables. The Charpy energy was acquired from the optical encoder signal and has been corrected for windage and friction in accordance with ASTM E23. The impact energy is the energy required to initiate and propagate a crack in the Charpy specimen. The optical encoder and the dial cannot correct for tossing energy or losses in the test machine, and therefore this small amount of additional energy, if present, may be included in the data for some tests. The instrumented striker energy does not include tossing energy or machine vibration energy since the energy, in this case, is measured only during a few milliseconds of contact between the striker and specimen. Based on comparison between the instrumented striker energy and the optical encoder energy, it has been shown that the tossing energy, and other losses, are small for most tests.

The lateral expansion is a measure of the transverse plastic deformation produced by the contact edge of the striker during the impact event. Lateral expansion is determined by measuring the maximum change of specimen thickness along the sides of the specimen. Lateral expansion is a measure of the ductility of the specimen. The nuclear industry tracks the embrittlement shift using the 35 mil (0.89 mm) lateral expansion index. In accordance with ASTM E23, the lateral expansion for some specimens, which could be broken after the impact test, should not be reported as broken since the lateral expansion of the unbroken specimen is less than that for the broken specimen. Therefore, when these conditions exist, the value listed is the unbroken measurement and a footnote is included to identify these specimens. All of the 177 degree capsule specimens that did not separate during the test could be broken by hand under the ASTM E23 requirements.

The percentage of shear fracture area is a direct quantification of the transition in the fracture modes as the temperature increases. All metals with a body centered cubic lattice structure, such as ferritic pressure vessel materials, undergo a transition in fracture modes. At low test temperatures, a crack propagates in a brittle manner and cleaves across the grains. As the temperature increases, the percentage of shear (or ductile) fracture increases. This temperature range is referred to as the transition region and the fracture process is mixed mode. As the temperature increases further, the fracture process is eventually completely ductile (i.e., no brittle component) and this temperature range is referred to as the upper shelf region.

Table 4-1
 Irradiated Charpy V-Notch Impact Test Results for Surveillance Base Metal
 Specimens (Heat C2557-1) from the Perry 177° Surveillance Capsule

Base Irradiated 177° Capsule							
Specimen ID	Test Temperature		Impact Energy		Lateral Expansion		Percent Shear (%)
	°F	(°C)	ft-lb	(J)	mils	(mm)	
BP1-B-7	-80.5	(-62.5)	3.74	(5.07)	0.9	(0.02)	1.3
BP1-B-8	-55.1	(-48.4)	6.68	(9.06)	4.0	(0.10)	3.1
BP1-B-11	-17.5	(-27.5)	15.85	(21.49)	11.3	(0.29)	9.4
BP1-B-9	10.2	(-12.1)	19.69	(26.70)	20.4	(0.52)	19.1
BP1-B-10	40.1	(4.5)	26.84	(36.39)	19.7	(0.50)	21.6
BP1-B-12	55.9	(13.3)	36.7	(49.76)	35.6	(0.90)	31.7
BP1-B-1	69.4	(20.8)	59.34	(80.45)	49.6	(1.26)	36.3
BP1-B-2	113.9	(45.5)	83.7	(113.48)	60.4	(1.53)	62.3
BP1-B-3	157.1	(69.5)	108.23	(146.74)	72.7	(1.85)	89.9
BP1-B-4	200.5	(93.6)	119.74	(162.34)	72.3	(1.84)	100.0
BP1-B-5	277.2	(136.2)	109.29	(148.18)	79.3	(2.01)	100.0
BP1-B-6	352.9	(178.3)	105.05	(142.43)	77.5	(1.97)	100.0

Table 4-2

Irradiated Charpy V-Notch Impact Test Results for Surveillance Weld Metal Specimens (Heat 5P6214B) from the Perry 177° Surveillance Capsule

Weld Irradiated 177° Capsule							
Specimen ID	Test Temperature		Impact Energy		Lateral Expansion		Percent Shear (%)
	°F	(°C)	ft-lb	(J)	mils	(mm)	
WP2-W-6	-111.6	(-79.8)	4.83	(6.55)	2.4	(0.06)	1.9
WP2-W-7	-72.4	(-58.0)	9.08	(12.31)	6.0	(0.15)	6.2
WP2-W-10	-28.3	(-33.5)	16.07	(21.79)	12.6	(0.32)	12.1
WP2-W-8	0.7	(-17.4)	24.91	(33.77)	18.0	(0.46)	20.9
WP2-W-11	19.8	(-6.8)	45.25	(61.35)	34.0	(0.86)	38.9
WP2-W-9	36.1	(2.3)	38.32	(51.95)	32.0	(0.81)	42.6
WP2-W-1	64.6	(18.1)	58.91	(79.87)	48.9	(1.24)	60.8
WP2-W-2	100.4	(38.0)	72.79	(98.69)	59.6	(1.51)	88.8
WP2-W-3	126.1	(52.3)	87.57	(118.73)	67.8	(1.72)	94.1
WP2-W-12	180.1	(82.3)	88.66	(120.21)	75.4	(1.92)	99.7
WP2-W-4	227.8	(108.8)	99.82	(135.34)	81.1	(2.06)	100.0
WP2-W-5	325.4	(163.0)	96.22	(130.46)	74.6	(1.89)	100.0

Table 4-3

Irradiated Charpy V-Notch Impact Test Results for Surveillance HAZ Metal Specimens from the Perry 177° Surveillance Capsule

HAZ Irradiated 177° Capsule							
Specimen ID	Test Temperature		Impact Energy		Lateral Expansion		Percent Shear (%)
	°F	(°C)	ft-lb	(J)	mils	(mm)	
HP3-H-8	-121.5	(-85.3)	2.83	(3.84)	10.1	(0.26)	4.0
HP3-H-9	-61.6	(-52.0)	14.96	(20.28)	5.2	(0.13)	17.0
HP3-H-6	-20.6	(-29.2)	25.53	(34.61)	20.5	(0.52)	15.3
HP3-H-7	12.2	(-11.0)	33.3	(45.15)	25.9	(0.66)	27.1
HP3-H-10	39.2	(4.0)	46.17	(62.60)	35.4	(0.90)	41.4
HP3-H-11	52.7	(11.5)	52.13	(70.68)	38.8	(0.99)	78.3
HP3-H-1	64.8	(18.2)	71.21	(96.55)	52.3	(1.33)	58.7
HP3-H-2	100.2	(37.9)	91.77	(124.42)	63.0	(1.60)	96.2
HP3-H-12	121.5	(49.7)	110.8	(150.22)	67.9	(1.72)	98.4
HP3-H-3	142.5	(61.4)	119.54	(162.07)	87.7	(2.23)	100.0
HP3-H-4	226.4	(108.0)	120.49	(163.36)	70.0	(1.78)	100.0
HP3-H-5	327.4	(164.1)	107.97	(146.39)	70.8	(1.80)	100.0

Section 5: Charpy Test Results

5.1 Analysis of Impact Test Results

For analysis of the Charpy test data, the BWRVIP ISP has selected the hyperbolic tangent (tanh) function as the statistical curve-fit tool to model the transition temperature toughness data. A hyperbolic tangent curve-fitting program named CVGRAPH [9] was used to fit the Charpy V-notch energy and lateral expansion data. Analysis methodology (e.g., definition of upper fixed shelf and lower shelf) followed the BWRVIP conventions established for analysis of all ISP data [20, 21]. The impact energy curve-fits from CVGRAPH are provided in Figures 5-1 (plate heat C2557-1) and 5-2 (weld heat 5P6214B), and the lateral expansion curve-fits are shown in Figures 5-3 (plate heat C2557-1) and 5-4 (weld heat 5P6214B). Because HAZ results are not used in the BWRVIP ISP, the HAZ data were not fit.

For the analysis of Charpy energy test data, lower shelf energy was fixed at 2.5 ft-lbs (3.4 J). Upper shelf energy was fixed at the average of all test energies exhibiting shear greater than or equal to 95%, consistent with ASTM Standard E185-82 [3]. For analysis of the lateral expansion test data, the lower shelf was fixed at 1.0 mils; the fixed upper shelf was defined as the average of the lateral expansion test data points at the same test temperatures used to define the fixed upper shelf energy.

5.2 Irradiated Versus Unirradiated CVN Properties

Table 5-1 summarizes the T_{30} [30 ft-lb (41 J) Transition Temperature], $T_{35\text{mil}}$ [35 mil (0.89 mm) Lateral Expansion Temperature], T_{50} [50 ft-lb (68 J) Transition Temperature], and Upper Shelf Energy for the unirradiated and irradiated materials and shows the change (shift) from baseline values. The unirradiated values of T_{30} and T_{50} were taken from the CVGRAPH fits provided in Figures 2-4 and 2-5; the unirradiated values of $T_{35\text{mil}}$ were previously determined in [20, 21]. The irradiated values are from the index temperatures determined in Figures 5-1 through 5-4.

Table 5-2 provides a comparison of the measured shifts to predicted shifts for plate heat C2557-1 and weld heat 5P6214B. Predicted shift is based on the formula provided in Regulatory Position 1.1 of Reg. Guide 1.99 Rev. 2 [6] as shown in Note 2 to Table 5-2. The fluence was input as 1.08×10^{18} n/cm², as reported in Table 3-8 for the 177° capsule. For surveillance plate heat C2557-1, the measured shift is within the value expected (e.g., the measured shift is less

than predicted shift + margin). For surveillance weld heat 5P214B, the measured shift is greater than the predicted shift + margin.

Measured percent decrease in USE is presented in Table 5-3 and compared to the percent decrease predicted by Regulatory Position 1.2 and Figure 2 of Reg. Guide 1.99, Rev. 2. For both the surveillance plate and weld, the measured percent decrease is less than the predicted percent decrease.

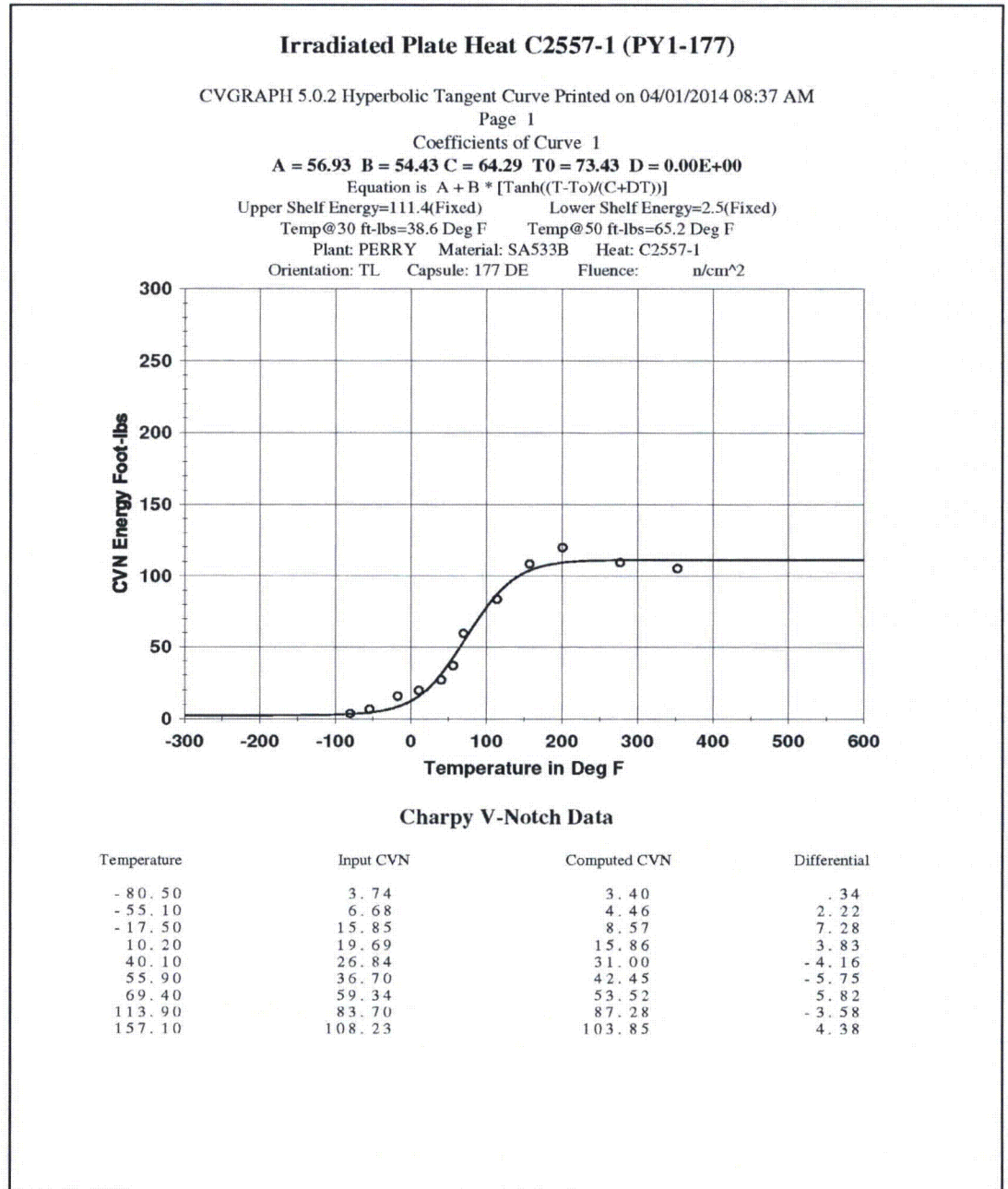


Figure 5-1
Irradiated Plate Heat C2557-1 Charpy Energy Plot (Perry 177° Capsule)

Irradiated Plate Heat C2557-1 (PY1-177)

Page 2

Plant: PERRY Material: SA533B Heat: C2557-1
Orientation: TL Capsule: 177 DE Fluence: n/cm²

Charpy V-Notch Data

Temperature	Input CVN	Computed CVN	Differential
200.50	119.74	109.31	10.43
277.20	109.29	111.17	-1.88
352.90	105.05	111.34	-6.29

Correlation Coefficient = .993

Figure 5-1 (continued)
Irradiated Plate Heat C2557-1 Charpy Energy Plot (Perry 177° Capsule)

Irradiated Weld Heat 5P6214B (PY1-177)

CVGRAPH 5.0.2 Hyperbolic Tangent Curve Printed on 04/01/2014 08:49 AM

Page 1

Coefficients of Curve 1

A = 48.7 B = 46.2 C = 85.82 T0 = 43.98 D = 0.00E+00

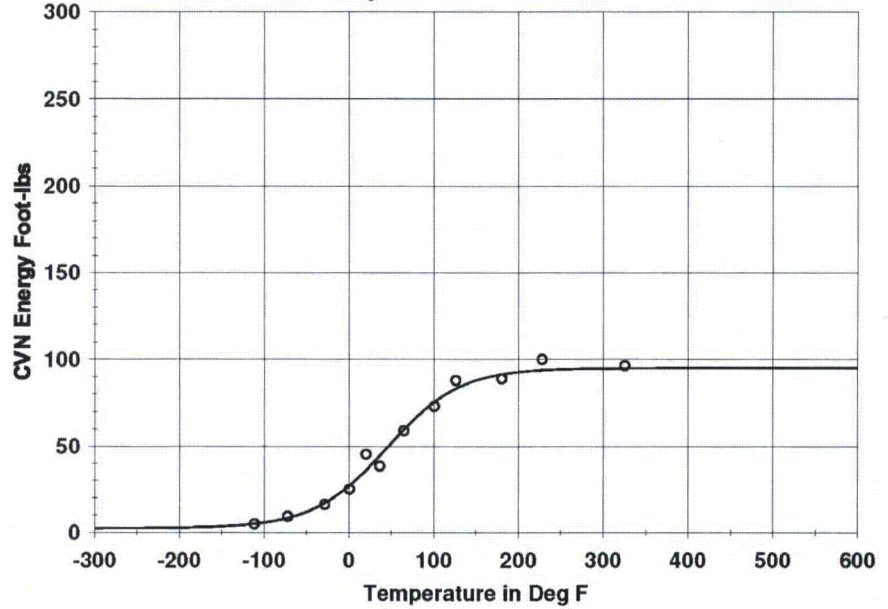
Equation is $A + B * [\text{Tanh}((T-T_0)/(C+DT))]$

Upper Shelf Energy=94.9(Fixed) Lower Shelf Energy=2.5(Fixed)

Temp@30 ft-lbs=7.2 Deg F Temp@50 ft-lbs=46.4 Deg F

Plant: PERRY AND SSP Material: SAW Heat: 5P6214B

Orientation: NA Capsule: 177 DE Fluence: n/cm²



Charpy V-Notch Data

Temperature	Input CVN	Computed CVN	Differential
-111.60	4.83	4.90	-.07
-72.40	9.08	8.25	.83
-28.30	16.07	16.96	-.89
7.70	24.91	27.20	-2.29
19.80	45.25	36.02	9.23
36.10	38.32	44.47	-6.15
64.60	58.91	59.59	-.68
100.40	72.79	75.34	-2.55
126.10	87.57	83.02	4.55

Figure 5-2
Irradiated Weld Heat 5P6214B Charpy Energy Plot (Perry 177° Capsule)

Irradiated Weld Heat 5P6214B (PY1-177)

Page 2

Plant: PERRY AND SSP Material: SAW Heat: 5P6214B
Orientation: NA Capsule: 177 DE Fluence: n/cm²

Charpy V-Notch Data

Temperature	Input CVN	Computed CVN	Differential
180.10	88.66	91.18	-2.52
227.80	99.82	93.64	6.18
325.40	96.22	94.77	1.45

Correlation Coefficient = .993

Figure 5-2 (continued)
Irradiated Weld Heat 5P6214B Charpy Energy Plot (Perry 177° Capsule)

Irradiated Weld Heat C2557-1 LE (PY1-177)

CVGRAPH 5.0.2 Hyperbolic Tangent Curve Printed on 04/01/2014 09:11 AM

Page 1

Coefficients of Curve 1

A = 38.7 B = 37.7 C = 73.43 T0 = 60.57 D = 0.00E+00

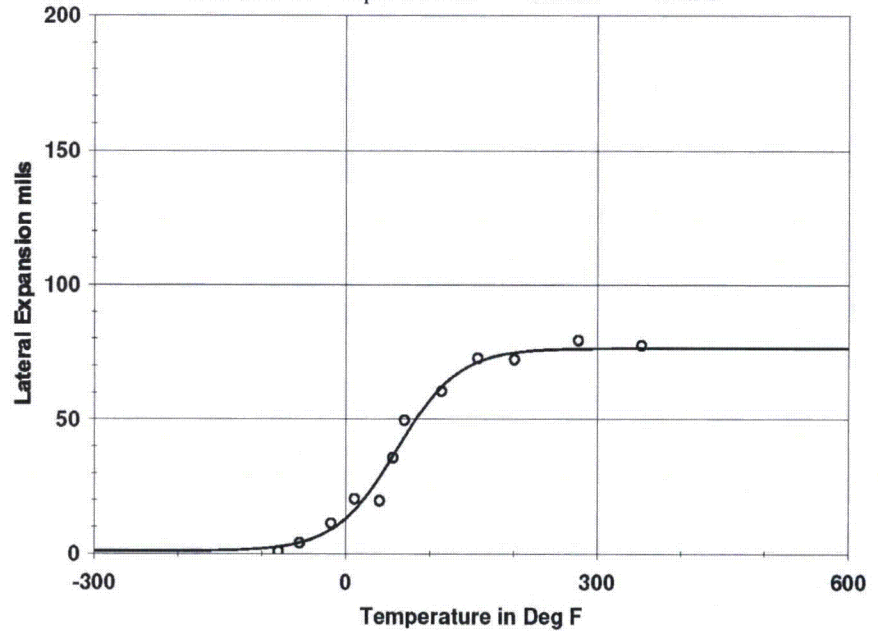
Equation is $A + B * [\text{Tanh}((T-T_0)/(C+DT))]$

Upper Shelf L.E.=76.4(Fixed) Lower Shelf L.E.=1.0(Fixed)

Temp.@L.E. 35 mils=53.4 Deg F

Plant: PERRY Material: SA533B Heat: C2557-1

Orientation: TL Capsule: 177 DE Fluence: n/cm²



Charpy V-Notch Data

Temperature	Input L.E.	Computed L.E.	Differential
- 80.50	.90	2.58	- 1.68
- 55.10	4.00	4.10	- .10
- 17.50	11.30	9.03	2.27
10.20	20.40	16.25	4.15
40.10	19.70	28.45	- 8.75
55.90	35.60	36.30	- .70
69.40	49.60	43.21	6.39
113.90	60.40	62.10	- 1.70
157.10	72.70	71.33	1.37

Figure 5-3
Irradiated Plate C2557-1 Lateral Expansion Plot (Perry 177° Capsule)

Irradiated Weld Heat C2557-1 LE (PY1-177)

Page 2

Plant: PERRY Material: SA533B Heat: C2557-1
Orientation: TL Capsule: 177 DE Fluence: n/cm²

Charpy V-Notch Data

Temperature	Input L.E.	Computed L.E.	Differential
200.50	72.30	74.77	-2.47
277.20	79.30	76.19	3.11
352.90	77.50	76.37	1.13

Correlation Coefficient = .992

Figure 5-3 (continued)
Irradiated Plate C2557-1 Lateral Expansion Plot (Perry 177° Capsule)

Irradiated Weld Heat 5P6214B LE (PY1-177)

CVGRAPH 5.0.2 Hyperbolic Tangent Curve Printed on 04/01/2014 09:09 AM

Page 1

Coefficients of Curve 1

A = 39. B = 38. C = 83.57 T0 = 44.11 D = 0.00E+00

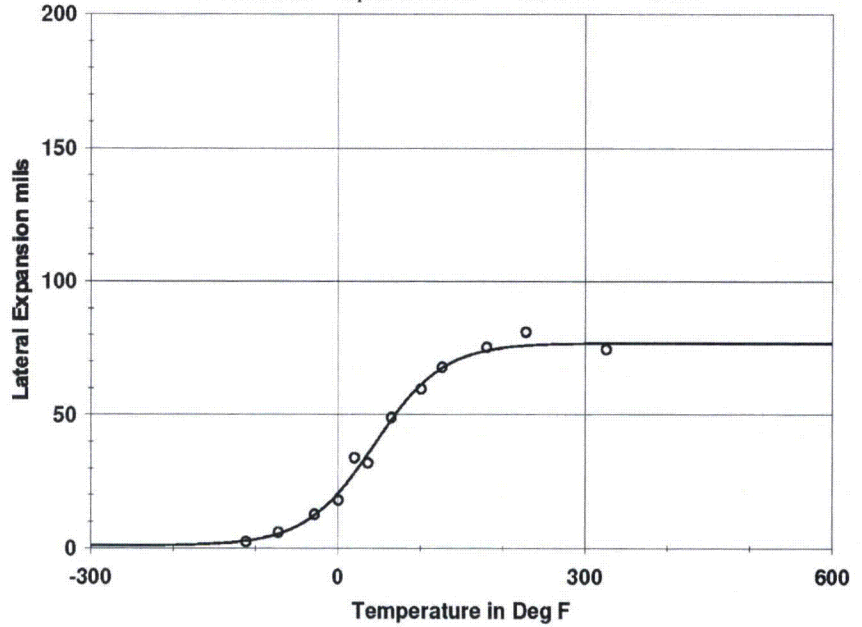
Equation is $A + B * [\text{Tanh}((T-T_0)/(C+DT))]$

Upper Shelf L.E.=77.0(Fixed) Lower Shelf L.E.=1.0(Fixed)

Temp.@L.E. 35 mils=35.3 Deg F

Plant: PERRY AND SSP Material: SAW Heat: 5P6214B

Orientation: NA Capsule: 177 DE Fluence: n/cm²



Charpy V-Notch Data

Temperature	Input L.E.	Computed L.E.	Differential
-111.60	2.40	2.79	-.39
-72.40	6.00	5.40	.60
-28.30	12.60	12.42	.18
.70	18.00	20.86	-2.86
19.80	34.00	28.25	5.75
36.10	32.00	35.37	-3.37
64.60	48.90	48.14	.76
100.40	59.60	61.32	-1.72
126.10	67.80	67.64	.16

Figure 5-4
Irradiated Weld Heat 5P6214B Lateral Expansion Plot (Perry 177° Capsule)

Irradiated Weld Heat 5P6214B LE (PY1-177)

Page 2

Plant: PERRY AND SSP Material: SAW Heat: 5P6214B
Orientation: NA Capsule: 177 DE Fluence: n/cm²

Charpy V-Notch Data

Temperature	Input L.E.	Computed L.E.	Differential
180.10	75.40	74.18	1.22
227.80	81.10	76.07	5.03
325.40	74.60	76.91	-2.31

Correlation Coefficient = .995

Figure 5-4 (continued)
Irradiated Weld Heat 5P6214B Lateral Expansion Plot (Perry 177° Capsule)

Table 5-1
Effect of Irradiation ($E > 1.0$ MeV) on the Notch Toughness Properties

Material Identity	T ₃₀ , 30 ft-lb (40.7 J) Transition Temperature			T ₅₀ , 50 ft-lb (67.8 J) Transition Temperature			T _{35mil} , 35 mil (0.89 mm) Lateral Expansion Temperature			CVN Upper Shelf Energy (USE)		
	Unirrad °F (°C)	Irradiated °F (°C)	ΔT ₃₀ °F (°C)	Unirrad °F (°C)	Irradiated °F (°C)	ΔT ₅₀ °F (°C)	Unirrad °F (°C)	Irradiated °F (°C)	ΔT _{35 mil} °F (°C)	Unirrad ft-lb (J)	Irradiated ft-lb (J)	Change ft-lb (J)
C2557-1 (TL orientation)	18.5	38.6	20.1	56.8	65.2	8.4	35.6	53.4	17.8	85.7	111.4	25.7
	(-7.5)	(3.7)	(11.2)	(13.8)	(18.4)	(4.7)	(2.0)	(11.9)	(9.9)	(116.2)	(151.0)	(34.8)
5P6214B	-33.2	7.2	40.4	2.7	46.4	43.7	-2.9	35.3	38.2	90.9	94.9	4.0
	(-36.2)	(-13.8)	(22.4)	(-16.3)	(8.0)	(24.3)	(-19.4)	(1.8)	(21.2)	(123.2)	(128.7)	(5.4)

Table 5-2
Comparison of Actual Versus Predicted Embrittlement

Identity	Material	Fluence (E>1.0 MeV, $\times 10^{17}$ n/cm ²)	Measured Shift ¹		RG 1.99 Rev. 2 Predicted Shift ²		RG 1.99 Rev. 2 Predicted Shift+Margin ^{2,3}	
			°F	(°C)	°F	(°C)	°F	(°C)
C2557-1 (TL)	Perry surveillance plate	10.8	20.1	(11.2)	13.4	(7.4)	26.8	(14.9)
5P6214B	Perry surveillance weld	10.8	40.4	(22.4)	15.9	(8.8)	31.8	(17.7)

1. The measured shift is taken from Table 5-1.
2. Predicted shift = CF \times FF, where CF is a Chemistry Factor taken from tables from USNRC RG 1.99, Rev. 2 [6], based on each material's Cu/Ni content, and FF is Fluence Factor, $f^{0.28-0.10 \log f}$, where f = fluence in units of 10^{19} n/cm² (E > 1.0 MeV) specified.
3. Margin = $2\sqrt{(\sigma_i^2 + \sigma_\Delta^2)}$, where σ_i = the standard deviation on initial RT_{NDT} (which is taken to be 0°F), and σ_Δ is the standard deviation on Δ RT_{NDT} (28°F for welds and 17°F for base materials, except that σ_Δ need not exceed 0.50 times the mean value of Δ RT_{NDT}). Thus, margin is defined as 34°F for plate materials and 56°F for weld materials, or margin equals shift (whichever is less), per Reg. Guide 1.99, Rev. 2.

Table 5-3
Percent Decrease In Upper Shelf Energy

Identity	Material	Capsule	Fluence (E>1.0 MeV, $\times 10^{17}$ n/cm ²)	Measured Decrease in USE (%)	Predicted Decrease in USE ¹ (%)
C2557-1	Perry surveillance plate	177°	10.8	- ²	8.3
5P6214B	Perry surveillance weld	177°	10.8	- ²	9.9

1. Based on the equations for Figure 2 of Reg. Guide 1.99 Rev. 2 [6] as provided in Reg. Guide 1.162 [22].
2. Value less than zero.

Section 6: References

1. 10 CFR 50, Appendices G (Fracture Toughness Requirements) and H (Reactor Vessel Material Surveillance Program Requirements), Federal Register, Volume 60, No. 243, dated December 19, 1995.
2. American Society of Mechanical Engineers (ASME) Boiler and Pressure Vessel Code (Code), Section XI, "Rules for In service Inspection of Nuclear Power Plant Components," Nonmandatory Appendix G, Fracture Toughness Criteria for Protection Against Failure.
3. ASTM E185-82, *Standard Practice for Conducting Surveillance Tests for Light-Water Cooled Nuclear Power Reactor Vessels*, E706 (IF), ASTM Standards, Section 3, American Society for Testing and Materials, Philadelphia, PA, 1993.
4. *BWRVIP-86, Revision 1-A: BWR Vessel and Internals Project, Updated BWR Integrated Surveillance Program (ISP) Implementation Plan*. EPRI, Palo Alto, CA: 2012. 1025144.
5. 10 CFR 50, Appendix B, "Quality Assurance Criteria for Nuclear Power Plants and Fuel Reprocessing Plants."
6. U.S. NRC Regulatory Guide 1.99, "Radiation Embrittlement of Reactor Vessel Materials," Revision 2, May 1988.
7. "Guidelines for the Management of Materials Issues," NEI 03-08, Nuclear Energy Institute, Washington, DC, Latest Edition.
8. "Perry Unit 1 RPV Surveillance Materials Testing and Analysis," L. J. Tilly, GE Nuclear Energy, GE-NE-B1301793-01, November, 1996.
9. CVGRAPH, Hyperbolic Tangent Curve Fitting Program, Developed by ATI Consulting, Version 5.0.2, Revision 1, 3/26/02.
10. "Calculational and Dosimetry Methods for Determining Pressure Vessel Neutron Fluence," Nuclear Regulatory Commission Regulatory Guide 1.190, March 2001.
11. *BWRVIP-126: BWR Vessel Internals Project, RAMA Fluence Methodology Software, Version 1.0*. EPRI, Palo Alto, CA: 2003. 1007823.
12. Letter from William H. Bateman (U.S. NRC) to Bill Eaton (BWRVIP), Safety Evaluation of Proprietary EPRI Reports BWRVIP-114, -115, -117, and -121 and TWE-PSE-001-R-001, dated May 13, 2005.

13. Letter from Matthew A. Mitchell (U.S. NRC) to Rick Libra (BWRVIP), "Safety Evaluation of Proprietary EPRI Report BWR Vessel and Internals Project, Evaluation of Susquehanna Unit 2 Top Guide and Core Shroud Material Samples Using RAMA Fluence Methodology (BWRVIP-145)," dated February 7, 2008.
14. "BUGLE-96: Coupled 47 Neutron, 20 Gamma-Ray Group Cross Section Library Derived from ENDF/B-VI for LWR Shielding and Pressure Vessel Dosimetry Applications," RSICC Data Library Collection, DL2C-185, March 1996.
15. "VITAMIN-B6: A Fine-Group Cross Section Library Based on ENDF/B-VI Release 3 for Radiation Transport Applications," RSICC Data Library Collection, DL2C-184, December 1996.
16. *BWRVIP-114-A: BWR Vessel and Internals Project, RAMA Fluence Methodology Theory Manual*, EPRI, Palo Alto, CA: 2009. 1019049.
17. *BWRVIP-121-A: BWR Vessel and Internals Project, RAMA Fluence Methodology Procedures Manual*, EPRI, Palo Alto, CA: 2009. 1019052.
18. G. C. Martin, Determination of Fast Neutron Density and Fluence: Duane Arnold Power Station, General Electric Company, December 6, 1977.
19. ASTM Standard E23, 2002, "Standard Test Methods for Notch Bar Impact Testing of Metallic Materials," ASTM International, West Conshohocken, PA, 2002, DOI: 10.1520/E0023-02, www.astm.org.
20. *BWRVIP-135, Revision 2: BWR Vessel and Internals Project, Integrated Surveillance Program (ISP) Data Source Book and Plant Evaluations*. EPRI, Palo Alto, CA: 2009. 1020231.
21. BWRVIP Letter 2010-238, Errata for BWRVIP-135, Rev. 2, October 15, 2010.
22. U.S. NRC Regulatory Guide 1.162, "Format and Content of Report for Thermal Annealing of Reactor Pressure Vessels," February 1996.

Appendix A: Dosimeter Analysis

A.1 Dosimeter Material Description

The Perry 177° surveillance capsule dosimeter materials are pure metal wires which were located within the surveillance capsule along the ends of the Charpy specimens. The wire types provided for the Perry surveillance program are iron and copper. Each wire is nominally about two inches (5.08 cm) long. Further discussion of the dosimeter cleaning and mass measurements follows.

A.2 Dosimeter Cleaning and Mass Measurement

At the time the surveillance capsule was opened, the dosimeter wires were cleaned in an ultrasonic cleaner and wiped with acetone wetted wipes to remove loose contamination. Upon receipt at the radiometric lab, the wires were visually inspected under a low magnification optical microscope. There was evidence of oxidation indicating the need for chemical etching and further cleaning. This was accomplished by soaking the Fe wire segments in a 4N solution of hydrochloric acid until the oxidation was etched from the surface. Similarly, the Cu wires were immersed in a 2N solution of nitric acid solution. The wires were then rinsed with distilled water, wiped once more with ethanol, and then allowed to dry in air at room temperature. The wires then exhibited a clean, shiny appearance. Figures A-1 through A-6 show low-power magnifications of the dosimetry wires as they were found prior to cleaning, and after cleaning and coiling.

The total mass of each wire was measured using a Mettler Toledo XS105DU analytical digital balance. Table A-1 lists the results of these measurements, as well as the identification assigned to each dosimeter. The dosimeter identifications were assigned as the type of dosimeter material followed by a numerical sequence number.

As previously mentioned, the wires were tightly coiled for subsequent counting and weighing. Each wire was wrapped around a thin metal rod to form a coil of approximately 0.5 inch (12.7 mm) diameter or less, which yields a reasonable approximation to a point source geometry at the distance the dosimeter wires are placed from the gamma detector. The coiled wire segments were pressed firmly against a hard surface to flatten the coil to yield the best counting geometry

A.3 Radiometric Analysis

Radiometric analysis was performed using high resolution gamma emission spectroscopy. In this method, gamma emissions from the dosimeter materials are detected and quantified using solid-state gamma ray detectors and computer-based signal processing and spectrum analysis. The specifications of the gamma ray spectrometer system (GRSS) are listed in Table A-2. The GRSS features a hyper pure germanium (HPGe) detector that is housed in a lead-copper shield to reduce background count rates. Standard background subtraction procedures were used.

GRSS calibration was performed using a National Institute for Standards and Technology (NIST) traceable mixed gamma quasi-point source. The Canberra analysis software provides the capability for energy resolution and efficiency calibration using specified standard source information. Calibration information is stored on magnetic disk for use by the spectrographic analysis software package.

Since detector efficiency depends on the source-detector geometry, a fixed-reproducible geometry must be selected for the gamma spectrographic analysis of the dosimeter materials. For the dosimeter wires, the counting geometry was that of a quasi-point source (coiled wire) placed five inches (12.7 cm) vertically from the top surface of the detector shell. In this way, extended sources up to 0.5 inch (1.27 cm) can be analyzed with a good approximation to a point source. The coiled wires were well within the area needed to approximate a point source geometry. The HPGe detector was calibrated for efficiency using the NIST traceable source. The accuracy of the efficiency calibration was checked using a gamma spectrographic analysis of the NIST traceable mixed gamma source. The isotopes contained in the source emit gamma rays which span the energy response of the detector for the dosimeter materials. These measurements show that the efficiency calibration is providing a valid measurement of source activity. The acceptance criteria for these measurements are that the software must yield a valid isotopic identification, and that the quantified activity of each correctly identified isotope must be within the uncertainty specified in the source certification. Validation of system performance was made prior to starting the counting tasks, and upon completion of all counting work for Perry. The counting system performance was acceptable in each case, indicating that the counting system properties did not change during the course of the counting procedure.

Table A-3 shows the counting schedule established for this work. There was no requirement for order of counting since the dosimeter materials still contained sufficient quantities of activation products to allow accurate radio assay. Counting times were more than sufficient to achieve the desired statistical accuracy for gamma emissions of interest in all cases.

Neutrons interact with the constituent nuclei of the dosimeter materials producing radionuclides in varying amounts depending on total neutron fluence, its energy spectrum, and the nuclear properties of the dosimeter materials. Table

A-4 lists the reactions of interest and their resultant radionuclide products for each element contained in the dosimeters. These are threshold reactions involving an n-p or n- α interaction.

Finally, Table A-5 presents the primary results of interest for flux and fluence determination. The specific activity units are in dps/mg, which normalizes the activity to dosimeter mass. The activities are specified for a useful reference date/time, which in this case is the Perry plant shutdown date and time. This reference date/time was specified as March 18, 2013, at 01:58:03 AM eastern standard time.

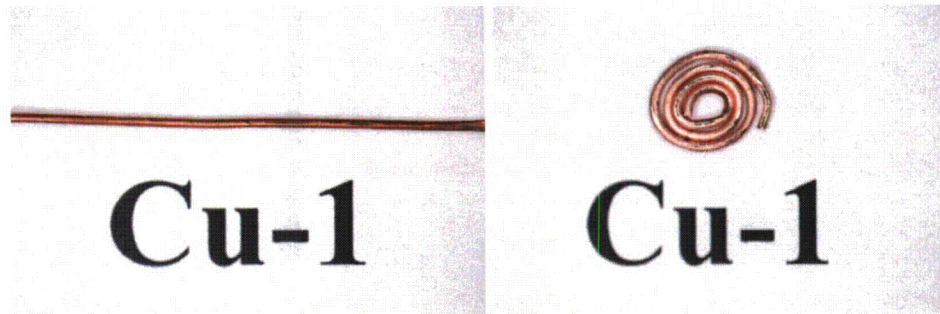


Figure A-1
Perry 177° Capsule Cu Dosimeter Wire Cu-1: Prior to Cleaning (left); and After
Cleaning/Coiling (right)

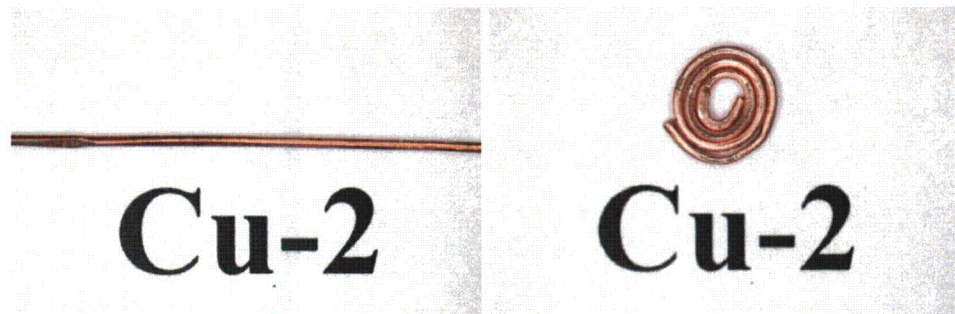


Figure A-2
Perry 177° Capsule Cu Dosimeter Wire Cu-2: Prior to Cleaning (left); and After
Cleaning/Coiling (right)

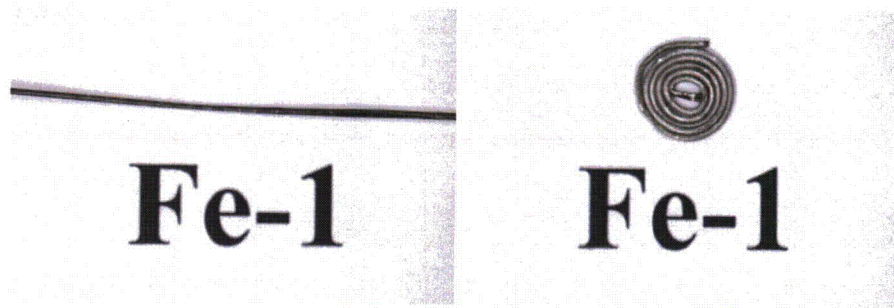


Figure A-3
 Perry 177° Capsule Fe Dosimeter Wire Fe-1: Prior to Cleaning (left); and After
 Cleaning/Coiling (right)

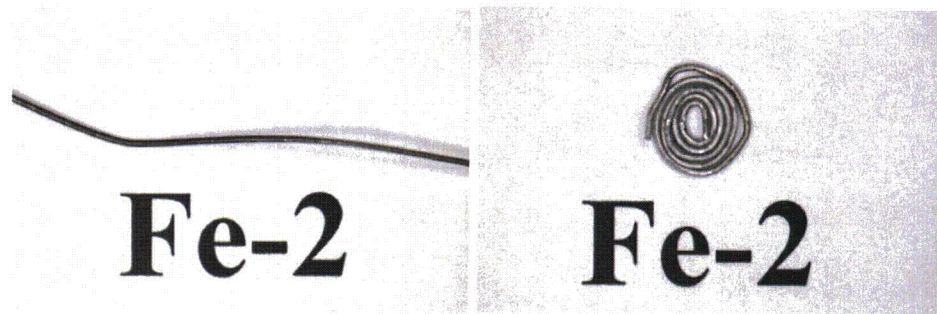


Figure A-4
 Perry 177° Capsule Fe Dosimeter Wire Fe-2: Prior to Cleaning (left); and After
 Cleaning/Coiling (right)

Table A-1
 Perry 177° Capsule Charpy Packet Dosimeter Wire Masses

Wire Dosimeter ID	Mass (mg)
Cu-1	224.53
Cu-2	225.91
Fe-1	131.20
Fe-2	128.47

Table A-2
Gamma Ray Spectrometer System (GRSS) Specifications

System Component	Description and/or Specifications
Detector	Canberra Model GC1518
Energy Resolution	1.8keV @ 1.33 MeV
Detector Efficiency Relative to a 3 inch x 3 inch NaI Crystal	15% at 1.3 MeV
Amplifier/Multichannel Analyzer	Canberra DAS-1000
Computer System	Intel i5-2500 CPU at 3.30 GHz,, 2.91 GB Main Memory, 931 GB Hard Disk, 17-inch Monitor, HP LaserJet Printer
Software	Canberra Apex v 1.2

Table A-3
Counting Schedule for Perry 177° Capsule Dosimeter Materials

Dosimeter ID	Count Start Date	Count Start Time (EST)	Count Duration (Live Time Seconds)
Cu-1	01/22/14	2:19 PM	86,400
Cu-2	01/23/14	3:37 PM	86,400
Fe-1	01/24/14	4:00 PM	86,400
Fe-2	01/27/14	12:26 AM	86,400

Table A-4
Neutron-Induced Reactions of Interest

Dosimeter Material	Neutron-Induced Reaction	Reaction Product Radionuclide
Iron	$Fe^{54}(n,p)Mn^{54}$	Mn^{54}
Copper	$Cu^{63}(n,\alpha)Co^{60}$	Co^{60}

Table A-5
 Results of Perry 177° Capsule Radiometric Analysis

Dosimeter ID	Isotope ID	Activity at Reference Date/Time ^a (μCi)	Specific Activity at Reference Date/Time ^a (dps/mg)	Activity Uncertainty (%)
Cu-1	⁶⁰ Co	1.53E-01	25.21	1.89
Fe-1	⁵⁴ Mn	4.70E-01	132.55	2.55
Cu-2	⁵⁸ Co	1.54E-01	25.22	1.89
Fe-2	⁵⁴ Mn	4.42E-01	127.30	2.56

^a March 18, 2013 at 01:58:03 AM EST is the reference date and time.

The Electric Power Research Institute, Inc. (EPRI, www.epri.com) conducts research and development relating to the generation, delivery and use of electricity for the benefit of the public. An independent, nonprofit organization, EPRI brings together its scientists and engineers as well as experts from academia and industry to help address challenges in electricity, including reliability, efficiency, affordability, health, safety and the environment. EPRI also provides technology, policy and economic analyses to drive long-range research and development planning, and supports research in emerging technologies. EPRI's members represent approximately 90 percent of the electricity generated and delivered in the United States, and international participation extends to more than 30 countries. EPRI's principal offices and laboratories are located in Palo Alto, Calif.; Charlotte, N.C.; Knoxville, Tenn.; and Lenox, Mass.

Together...Shaping the Future of Electricity

Programs:

Nuclear Power

BWR Vessel and Internals Project

© 2014 Electric Power Research Institute (EPRI), Inc. All rights reserved. Electric Power Research Institute, EPRI, and TOGETHER...SHAPING THE FUTURE OF ELECTRICITY are registered service marks of the Electric Power Research Institute, Inc.

3002003141

Electric Power Research Institute

3420 Hillview Avenue, Palo Alto, California 94304-1338 • PO Box 10412, Palo Alto, California 94303-0813 USA
800.313.3774 • 650.855.2121 • askepri@epri.com • www.epri.com